



Article

# Numerical and experimental investigations on a thermoelectric generator for electric power generation from waste heat recovery in a combined cycle power plant – an energy and economic (2E) analysis

Subbarama Kousik Suraparaju<sup>1,2,3,\*</sup>, Elavarasan Elangovan<sup>4</sup>, Gopi Vasudevan<sup>5</sup>, Mahendran Samykano<sup>2,3</sup> and Sendhil Kumar Natarajan<sup>5,\*</sup>

- <sup>1</sup> Solar Energy Laboratory, Department of Mechanical Engineering, Sri Vasavi Engineering College (A), Tadepalligudem, Andhra Pradesh – 534101, India.
  - <sup>2</sup> Centre for Research in Advanced Fluid and Process, Universiti Malaysia Pahang Al-Sultan Abdullah, Lebuhraya Tun Razak, Gambang, Kuantan 26300, Pahang, Malaysia.
  - <sup>3</sup> Faculty of Mechanical and Automotive Engineering Technology, Universiti Malaysia Pahang Al-Sultan Abdullah, 26600 Pekan, Pahang, Malaysia.
  - <sup>4</sup> Department of Aerospace Engineering, SJC Institute of Technology, Chikkaballapur, Karnataka 562101, India.
  - <sup>5</sup> Solar Energy Laboratory, Department of Mechanical Engineering, National Institute of Technology Puducherry, Karaikal, Union Territory of Puducherry – 609609, India.
- \* Correspondence: kousik.mech@srivasaviengg.ac.in, sendhil80@nitpy.ac.in

Received: 07 March 2024; Accepted: 15 November 2024; Published: 02 July 2025

**Abstract:** With the ever-growing population in the world, the electricity demand has elevated drastically over the decades. Several kinds of research are being carried out to meet the electricity needs of the world with conventional and non-conventional energy sources. The conventional form of generating electricity from power plants has lesser efficiency and there is always scope for increasing the efficiency of power plants by using several heat recovery methods. The efficacy of the combined cycle power plant is around 62% where more amount of energy is dissipated as waste heat. The main objective of this study is to utilize the waste heat for power generation by effective utilization of Thermo-Electric Generators (TEGs). Therefore, the 32.5 MW combined cycle power plant located in Karaikal is chosen for this study. The powerplant uses HRSG to recover and utilize the waste heat to generate steam using it for the steam turbine. The study mainly focuses on the deployment of TEGs in the powerplant to generate electricity using waste heat. In this regard, the numerical analysis of TEGs under different conditions has been analyzed and the best approach is chosen for experimental investigation. Further, an experimental prototype with similar operating conditions to a powerplant is developed and analyzed for the effect of TEGs in electric power generation. Finally, the cost-effectiveness of deploying TEGs in a power plant has been analyzed using economic analysis.

© 2025 by the authors. Published by Universidad Tecnológica de Bolívar under the terms of the [Creative Commons Attribution 4.0 License](https://creativecommons.org/licenses/by/4.0/). Further distribution of this work must maintain attribution to the author(s) and the published article's title, journal citation, and DOI. <https://doi.org/10.32397/tesea.vol6.n1.643>

## 1. Introduction

Electricity generation from waste heat employing thermoelectric generators has originated conceptually and experimentally since the 1980s. Thermoelectric generators are devices that directly convert heat into electricity using the Seebeck effect. They comprise many P and N-type elements that are connected electrically in series but thermally in parallel. The TEGs are more expensive and less efficient devices. The efficiency is increasing with every development and there is still scope for the development of TEGs to date [1–3]. Thermoelectric Generators are being used in various applications and their potentiality increasing day by day. Many parametric optimizations are being developed for the better performance of TEGs. In recent days many renewable energy applications are also utilizing these TEGs as TEG will boost the efficiency of the system [4–6]. The research of TEGs, one of the profound studies of TEGs stated that the TEGs could be effectively used to convert the waste heat into electricity. However, the conversion efficiency was low and also the efficiency was insignificant since the source of energy is economically free [7]. TEGs have been used for cooling applications in electronic devices over the past few years [8], and more recently used as refrigerators, water heaters, and also as large-scale applications to enhance the efficacy of Rankine cycle-based power plants [9–11]. An experimental setup was developed based on thermoelectricity and heat transfer and it was analyzed to predict the performance of TEGs for low-grade waste heat sources [12, 13]. The most commonly utilized material in commercial TEG accessories is Bismuth Telluride ( $\text{Bi}^2\text{Te}^3$ ).

Nevertheless, the maximum working temperature is 300 °C and the future costs and accessibility of Tellurium are indeterminate. As a repercussion of these circumstances, materials like Silicides, Skutterudites, and Oxides would be the future of thermoelectric materials [14, 15]. Duraiswami et al. and Orr et al. [16, 17] briefly explained the waste heat recovery from automobile exhaust. Furue et al. [18] determined that 184 kW of electricity could be recovered from the exhaust gas heat from the internal combustion engine of a capacity of 10MW. Kyono et al. [19] assessed that around 150 kW could be attained by employing TEGs in the vapor condenser of a steam power plant. Also, a TEG system was installed in the 25-kW carbon furnace at the Awazu plant of Komatsu Ltd., in which, the system consists of sixteen 50 x 50 mm<sup>2</sup> TEGs and produces up to 214 W of electrical energy when the temperature difference of 200°C across each TEGs [20]. A new waste heat recovery during the metal casting process with TEG was evolved and investigated mathematically and experimentally for its better performance [21]. William [22] depicted the advancement of a computationally effective computer-aided design (CAD) method using a finite element numerical model (FEM) associated with empirical correlations for the generation of optimized heat sink design. C.J Shih [23] showed a plate-fin heat sink of optimized design with horizontal inlet flow has a marginally improved performance than that with vertical inlet flow. In this contrast, a new marine waste heat recovery TEG was evolved in which it is investigated and optimized for better performance [24]. Kraemer et al. discussed thermoelectric generators with high thermal performance and the efficiency is increased enormously by using high-performance nanostructured thermoelectric materials and some choosy solar absorbers in a creative design that exploits high thermal concentration in an evacuated environment [25]. Other than this, many solar thermal-based applications are utilizing Thermoelectric generators for better

performance [26–28]. In the context of this study, the combined cycle power plant's operational efficiency is cited as approximately 62%. This figure is consistent with findings from recent literature that underscore the advancements in combined cycle technology. Knox et al. [11] note that contemporary systems can achieve efficiencies exceeding 60% under optimal operational conditions, particularly when integrating advanced technologies such as heat recovery steam generators (HRSGs)(TESEA). Furthermore, Champier [29] emphasizes that with appropriate engineering practices and system configurations, combined cycle power plants can achieve efficiencies of around 62%, showcasing their potential for significant energy recovery. The world is shifting towards recovering waste heat by using TEGs. The exhaust from the automobile is one of the most trending waste heat recovery process applications. Subsequently, space and nuclear applications are also using TEGs for better efficiency in waste heat recovery [30–36].

Based on the above literature, it is apparent that the application of TEGs for electric power generation using waste heat is a sustainable and viable approach. TEGs were specifically chosen for this study due to their unique ability to directly convert waste heat into electrical energy, offering a promising solution for enhancing energy efficiency in renewable energy systems. Given the growing global focus on sustainability and energy recovery, TEGs provide a reliable and maintenance-free option with no moving parts, ensuring durability and long-term operational stability. Additionally, their scalability and compatibility with various thermal energy sources make them highly versatile for a wide range of applications. The 32.5 MW combined cycle power plant in Karaikal was selected for this study due to several key factors that align with the objectives of the research. Firstly, this plant operates with Heat Recovery Steam Generators (HRSG), which offer an ideal setup for investigating waste heat recovery using Thermo-Electric Generators (TEGs). The significant amount of waste heat generated in the plant provided an excellent opportunity to test the efficacy of TEGs in converting this waste heat into usable electric power. Moreover, the plant's operational conditions, including its chimney wall temperature, height, and ambient conditions, were particularly suitable for the experimental and numerical analysis of TEG deployment. The availability of accurate operational data and access to the plant's infrastructure also allowed for the development of a realistic experimental prototype. Additionally, the Karaikal plant represents a mid-scale power facility, making it ideal for assessing the economic feasibility and scalability of implementing TEGs in similar combined cycle plants. These considerations made the Karaikal plant a fitting choice for this study, contributing to the practical and theoretical value of the research.

Hence, in the current study, the 32.5 MW combined cycle power plant of Puducherry Power Corporation Limited (PPCL), located in Karaikal, India, is chosen for analyzing the effect of TEGs in electric power generation using waste heat that is recovered from HRSG. The effect of TEGs with different configurations has been analyzed numerically and experimentally in this study. Finally, the cost-effectiveness of deploying TEGs in a power plant is analyzed using economic analysis.

## 2. Numerical Analysis

### 2.1. Simulation Parameters & Assumptions

The design and simulation of the whole scenario of using the thermoelectric generator on a powerplant's chimney wall to recover the waste heat were done using SOLIDWORKS. For the simulations to be carried out, the following parameters are considered:

- **Chimney's wall temperature:** Measured at 180 °C using an infrared thermometer.
- **Chimney's height:** Obtained from the layout provided by the power plant administration.
- **Convective heat transfer coefficient:** Calculated based on the flow conditions, with a value determined to be 40.25 W/m<sup>2</sup>.

- **Average wind velocity:** Assumed to be 10 m/s for forced convection conditions.
- **Average ambient temperature:** Set at 30 °C.

The wall temperature of the chimney was measured with the help of an infrared thermometer. The wall temperature was found to be 180 °C. The height of the chimney was obtained from the layout provided by the power plant administration. The chimney was insulated only up to a certain height and insulation-free for the rest of the portion. Hence, TEG is proposed to be placed insulation-free region where even paint is scraped off to ensure better heat conduction between TEG and the chimney wall. The convective heat transfer coefficient was calculated using the required formulas considering the flow to be external forced flow over a flat plate.

The design and simulation of the whole scenario of using the thermoelectric generator on a power plant's chimney wall to recover the waste heat were done using SOLIDWORKS. For the simulations to be carried out, the following assumptions were considered:

### Assumptions:

1. The TEG module is assumed to be in full contact with the chimney wall.
2. There is no paint or insulation present at the TEG installation sites, facilitating better heat conduction.
3. The flow is considered to be forced convective flow over a flat plate, with no standstill air at any time.
4. It is assumed that there is no contact resistance between the chimney wall and TEG, ensuring optimal thermal transfer.

### 2.2. Simulation Results

Situation 1: The thickness of TEG is equal to 4 mm

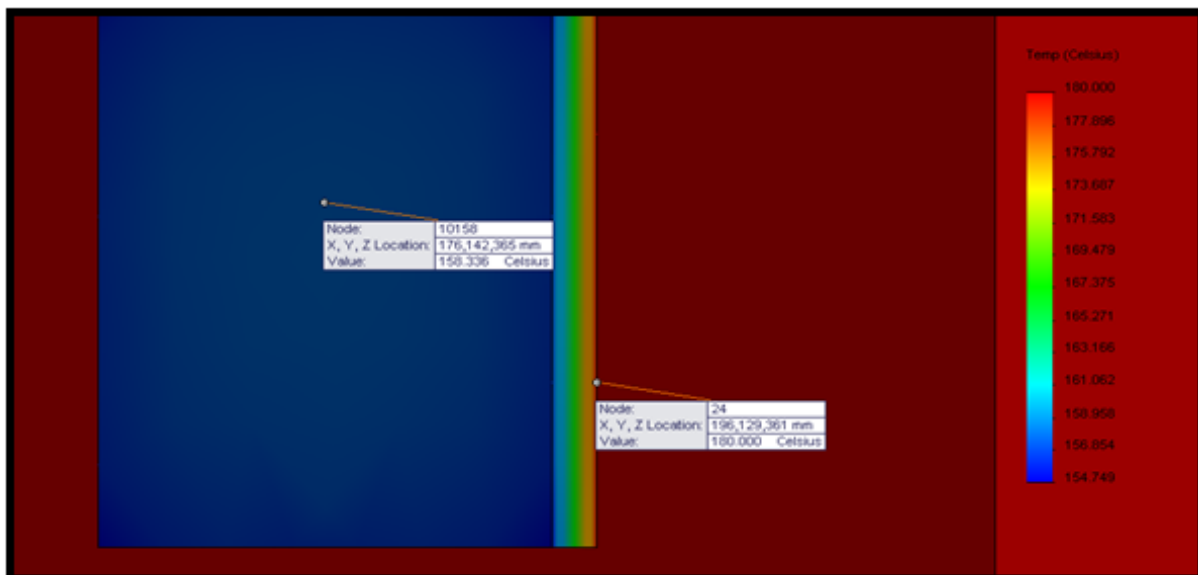


**Figure 1.** Four (4) mm thick TEG.

From Figure 1, it is observed that using a TEG with a thickness of 4 mm resulted in a temperature difference of 22 °C.

Situation 2: The thickness of the TEG is equal to 6 mm

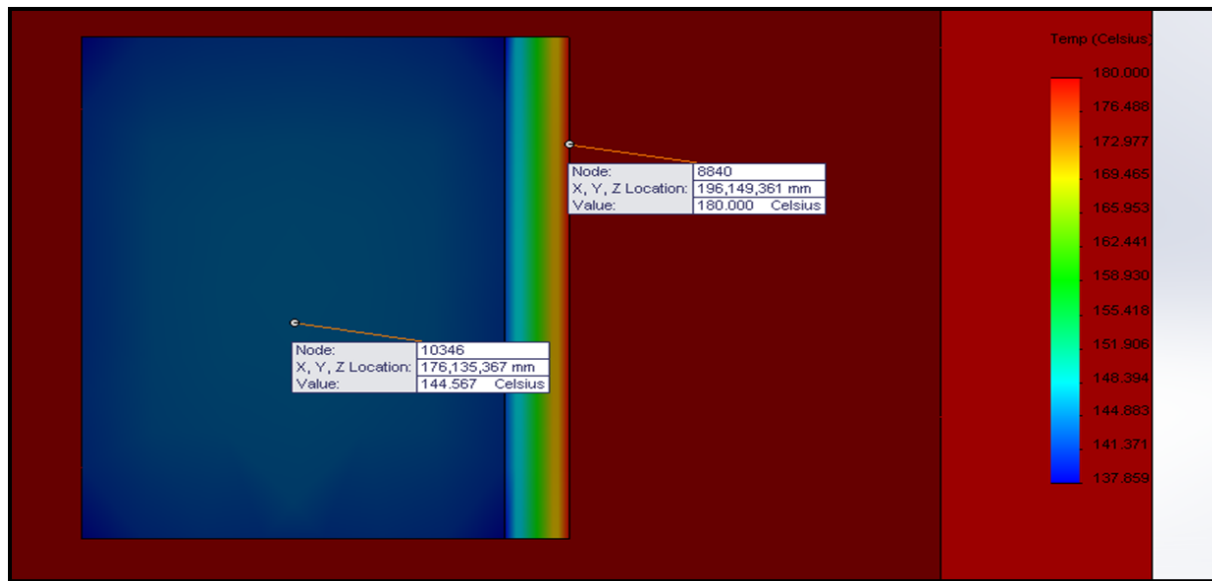


Figure 2. Six (6) mm thick TEG.

From Figure 2, it is observed that using a TEG with a thickness of 6 mm resulted in a temperature difference of 36 °C.

Situation 3: The thickness of TEG is equal to 8 mm

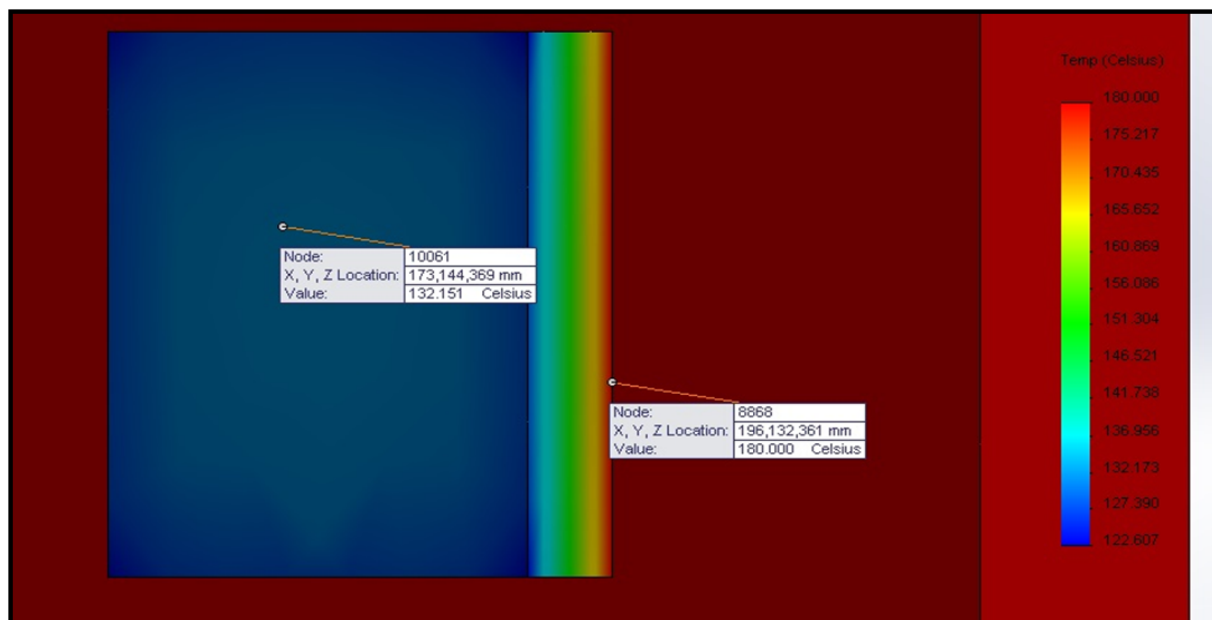


Figure 3. Eight (8) mm thick TEG.

From Figure 3, it is observed that using a TEG with a thickness of 8 mm resulted in a temperature difference of 48 °C.

Situation 4: The thickness of TEG is equal to 4 mm with fins

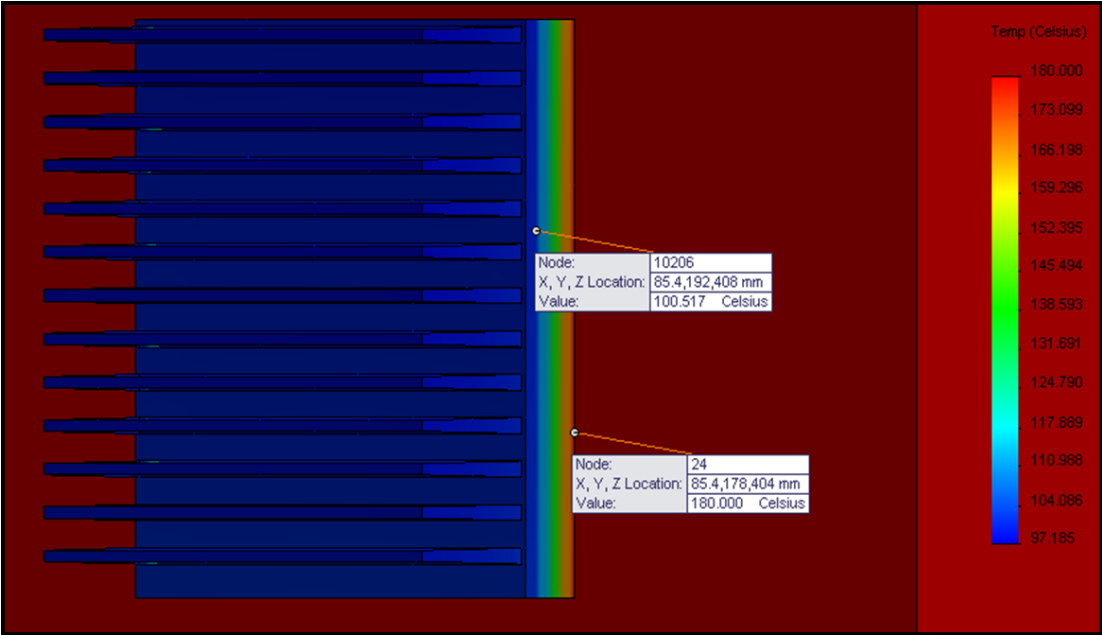


Figure 4. Four (4) mm thick TEG with Fins.

From Figure 4, it is observed that using a 4 mm thick TEG with fins to enhance convection losses the temperature difference can be increased appreciably, which is equal to 80 °C.

Situation 5: The thickness of TEG is equal to 6 mm with fins

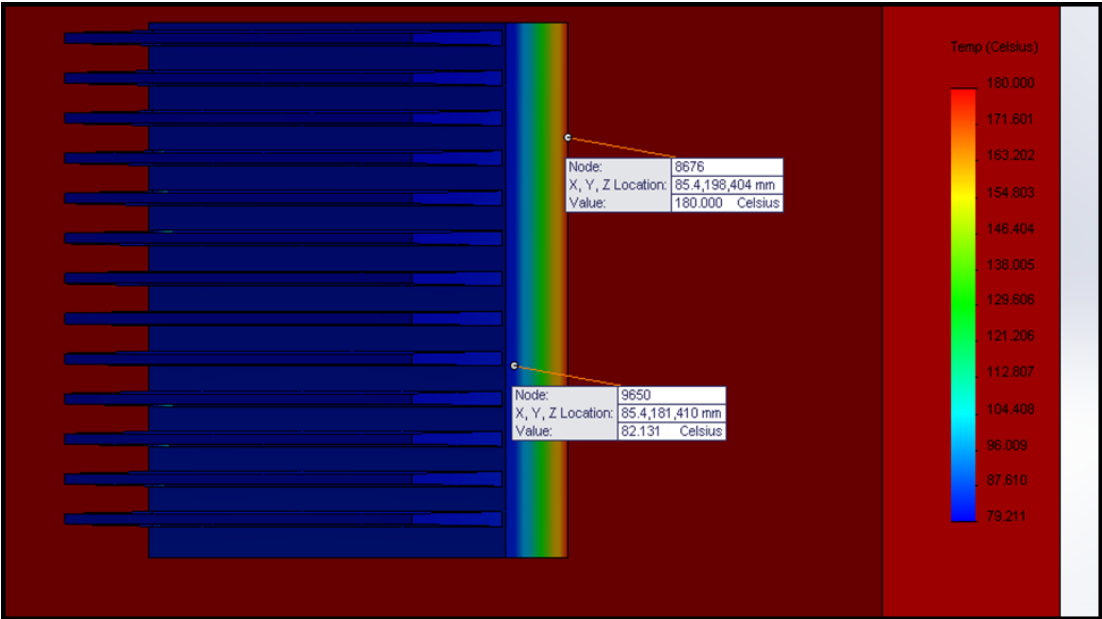
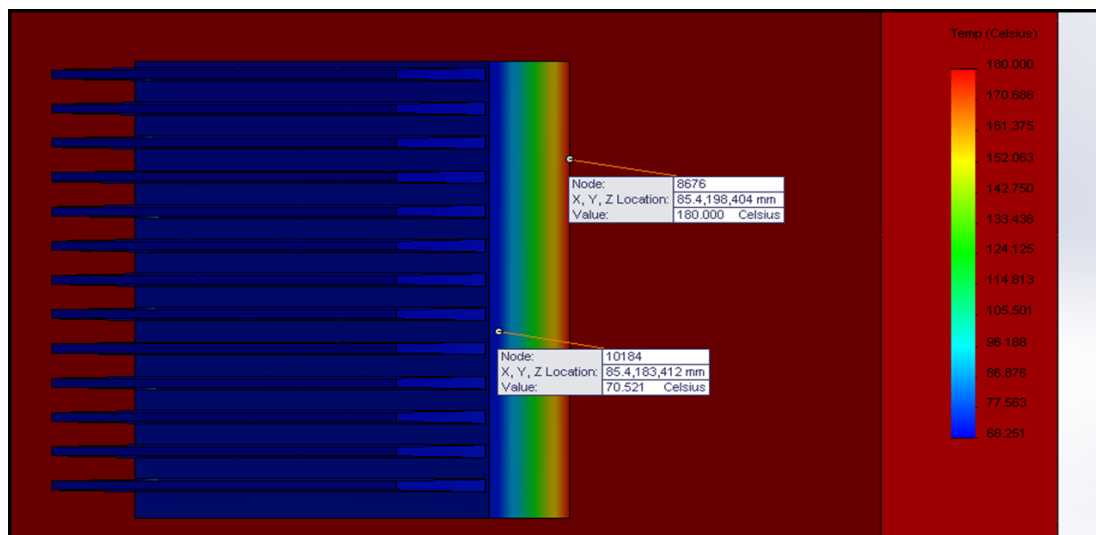


Figure 5. Six (6) mm TEG with Fins.

From Figure 5, it is observed that using a 6 mm thick TEG with fins to enhance convection losses the temperature difference can be increased appreciably, which is equal to 98 °C.

Situation 6: The thickness of TEG is equal to 8 mm and with fins



**Figure 6.** Eight (8) mm TEG with fins.

From Figure 6, it is observed that using an 8mm thick TEG with fins to enhance convection losses the temperature difference can be increased appreciably, which is equal to 110 °C.

From the above situations, it is apparent that as the thickness of the TEG is increased the temperature difference also increases, which ultimately will increase the power production. This phenomenon is mainly due to the decrease in thermal conductivity. So, a TEG with 8 mm will be a good choice for installation since it's commercially available and also because considering a TEG with more thickness than 8mm will result in compromising the robustness, compactness, and other advantages of a TEG. Also, using fins on TEGs can increase the temperature difference drastically hence improving power output with just an expense of an increase in weight of 127 grams.

### 3. Power Generation

Thermoelectric modules based on Bismuth Telluride were designed initially for only cooling or combined cooling and heating operations where electrical power generates a temperature difference across the module. By utilizing the modules “in reverse,” a temperature differential is applied across the module faces, and it is possible to generate electricity. Although generation and output efficiency are very low, beneficial power often may be attained where a source of heat is accessible.

#### 3.1. MATLAB program for calculation

A MATLAB program was written for better calculation of the TEG model at various cold temperatures. “High Power” thermoelectric module for generator operations is usually preferable to lessen the total system cost. For this purpose, a 127 couple, a 6-Ampere module is opted and to be used in the design.

##### 3.1.1. Results for power generation

From the simulation analysis of temperatures ranging from 323K to 422K, these results were considered. The results are tabulated in Table 1.

**Table 1.** Considered results as per the simulation analysis.

TEG Thickness	$T_c$	$T_{avg}$	$\Delta T$	$S_n$	$K_n$	$R_n$	$P_{max}$
<b>Parameters with Consideration of Fins on the Surface</b>							
8mm	343	398	110	0.051271	0.921237	3.543403	28.17711
6mm	355	404	98	0.05076	0.955082	3.603438	22.29261
4mm	373	413	80	0.049765	1.011192	3.687745	14.61286
<b>Parameters Without Consideration of Fins on the Surface</b>							
8mm	405	429	48	0.047262	1.127757	3.816592	4.91047
6mm	417	435	36	0.046062	1.177341	3.856647	2.651233
4mm	422	437.5	31	0.045518	1.198987	3.871838	1.923704

where,

- $T_c$  = Temperature of Colder Surface
- $\Delta T$  = Temperature difference
- $T_{avg}$  is the average module temperature in K
- $K$  is the module thermal conductance in Watts/K
- $S_n$  is the Seebeck coefficient for the new module
- $R_n$  is the new module’s electrical resistance
- $K_n$  is the new module thermal conductance
- $P_{max}$  is the maximum power that can be generated by a single module of TEG

3.1.2.  $P_{max}$  v/s  $T_c$  MATLAB Graph

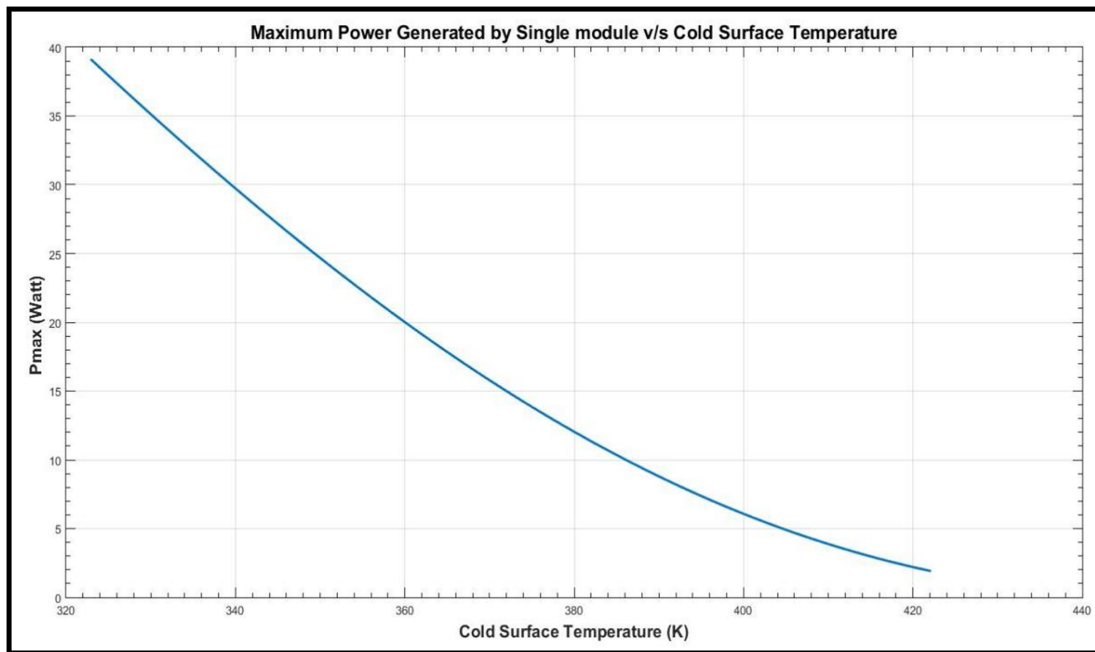


**Figure 7.**  $P_{max}$  v/s  $T_c$ .

From the results in Figure 7, it is evident that the attachment of fins to the cold side of TEG increases the  $\Delta T$  and hence the power is generated.

## 4. Numerical Analysis of Fins

### 4.1. Assumptions for Numerical Analysis

- The ambient temperature is to be 30 °C.
- There will be no standstill air at any time, i.e., it will be a forced convection situation with an air velocity of 4.167 m/s.
- The TEG module is in full contact with the chimney wall.
- There will be no paint on the TEG installation spots.
- The TEG and wall bond is perfect, i.e., no air pocket and remains the same until TEG’s removal.
- The surface of the cylinder is considered to be flat.
- No contact resistance is considered between the chimney wall & TEG and fins & TEG.
- Flow is considered to be forced convective flow over a flat plate.

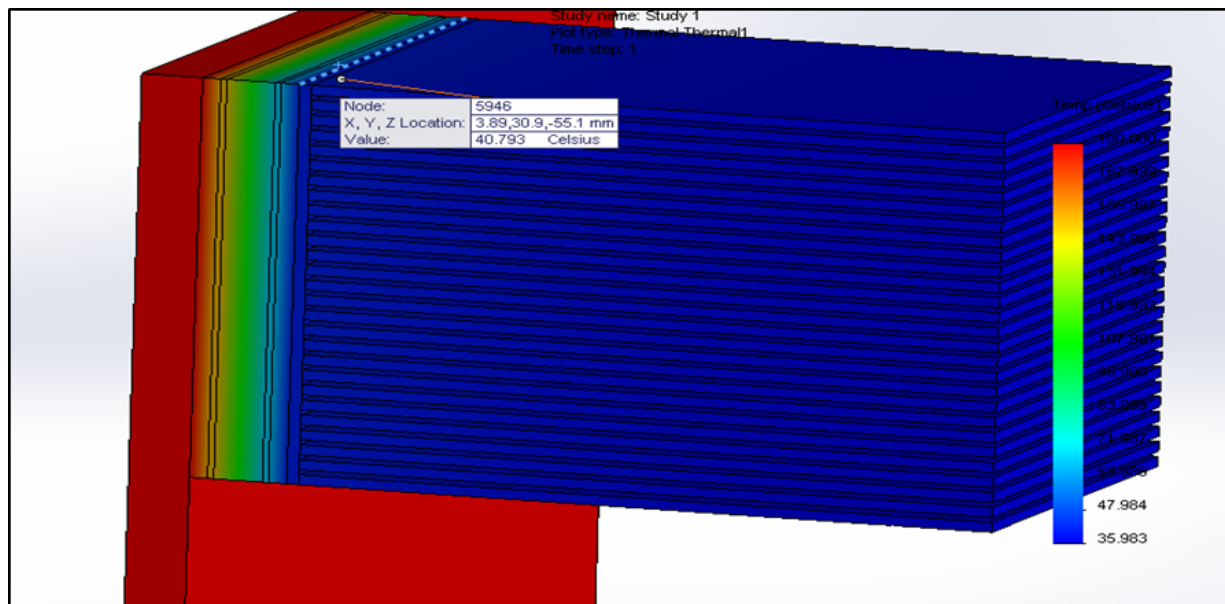
### 4.2. Parameters considered for the simulation

- Ambient temperature = 30 °C,
- Convective heat transfer coefficient = 41 W/m<sup>2</sup>K,
- Bismuth Telluride TEG pellets and Ceramic porcelain substrate.

### 4.3. Simulation Results

Situation 1: Fin Thickness = 1 mm and Fin height = 57.40 mm

At z (fin spacing) = 0.5 mm



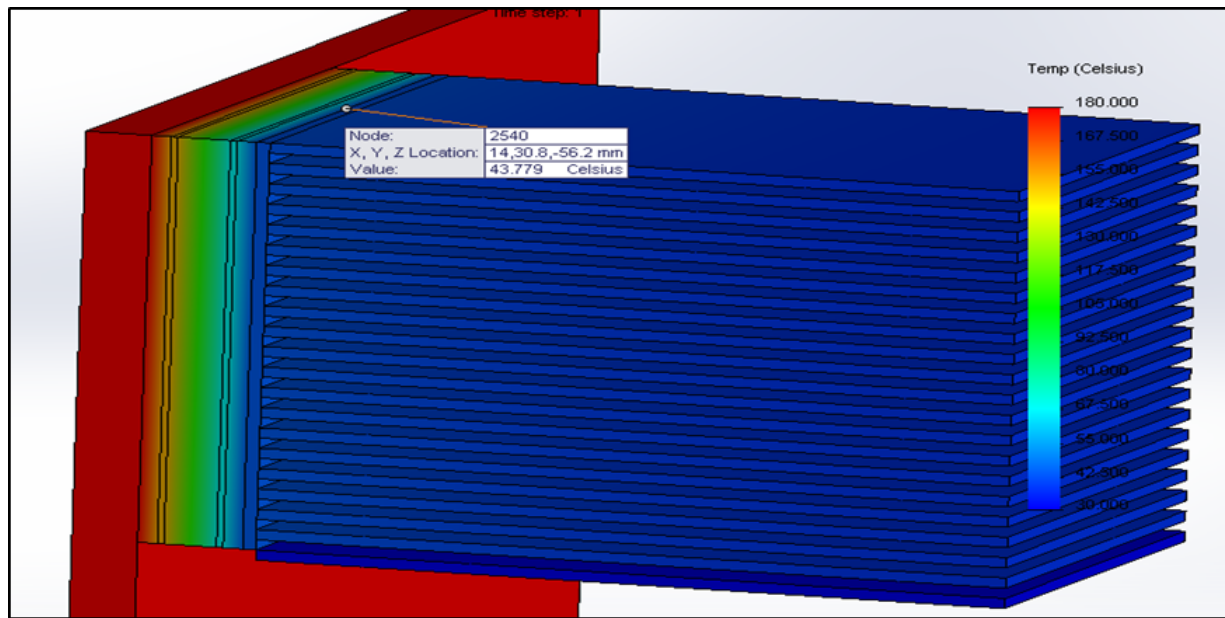


Figure 9. At z = 1mm.

Situation 2: Fin thickness = 0.9 mm and Fin height = 54 mm

At z = 0.5 mm

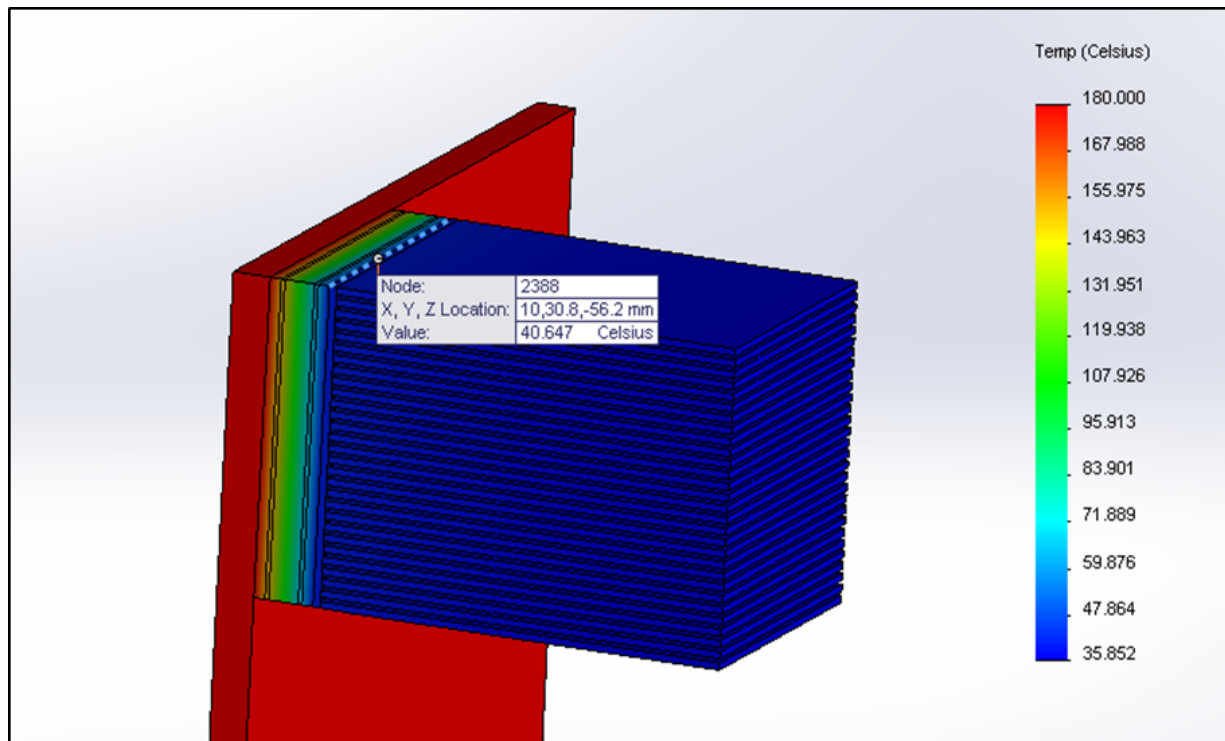


Figure 10. At z = 0.5mm.

For fin spacing of 0.5 mm,  $\Delta T$  came out to be 140 °C as shown in Figure 10.  
At z = 1 mm

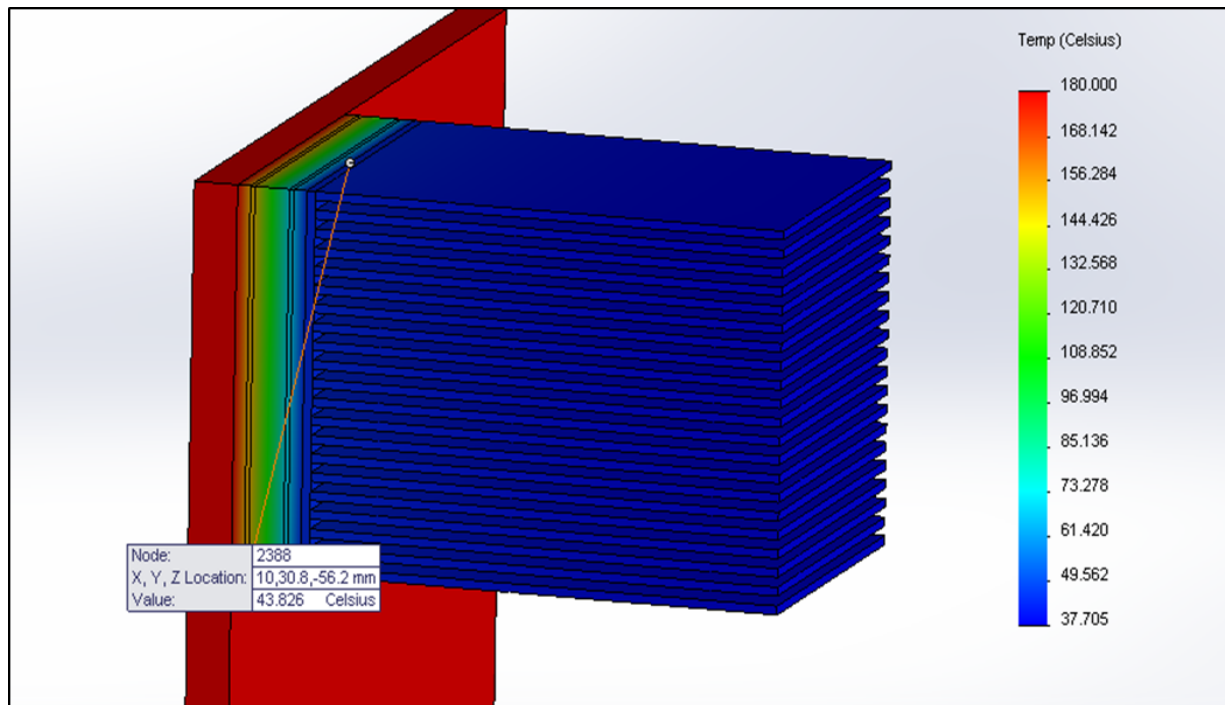


Figure 11. At z = 1mm.

For fin spacing of 1 mm,  $\Delta T$  came out to be 136 °C as shown in Figure 11.

Situation 3: Fin thickness = 0.7 mm and Fin height = 48 mm

At z = 0.5 mm

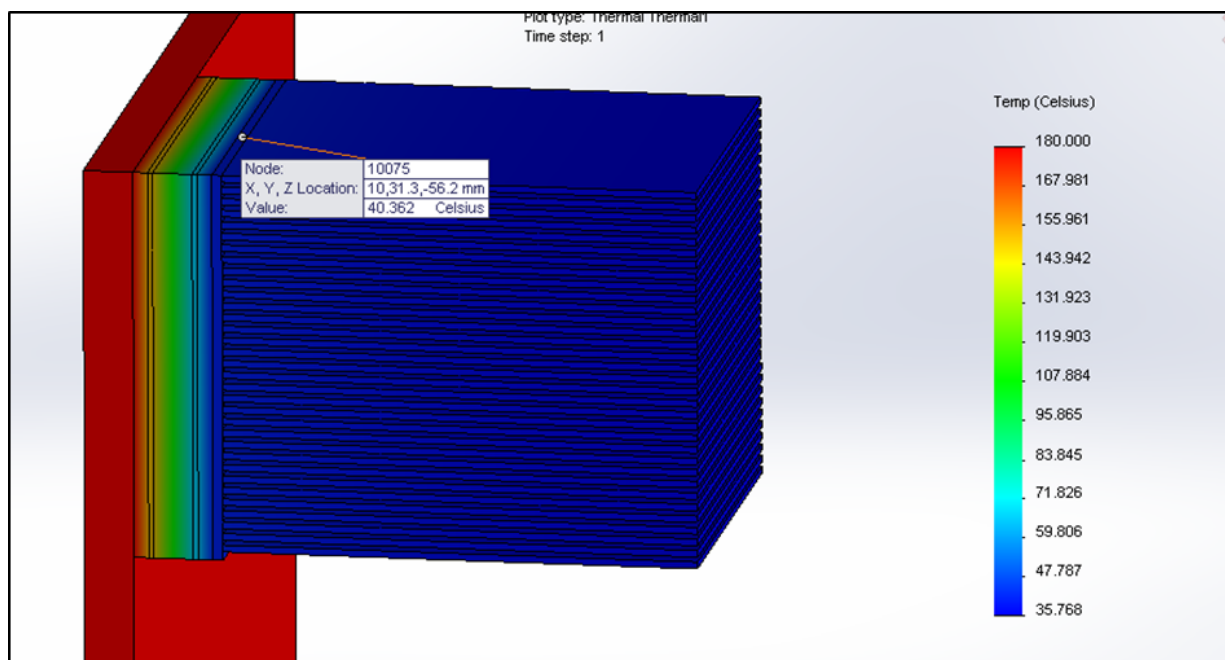


Figure 12. At z = 0.5mm.

For fin spacing of 0.5 mm,  $\Delta T$  came out to be 140 °C as shown in Figure 12.  
 At  $z = 0.7$  mm

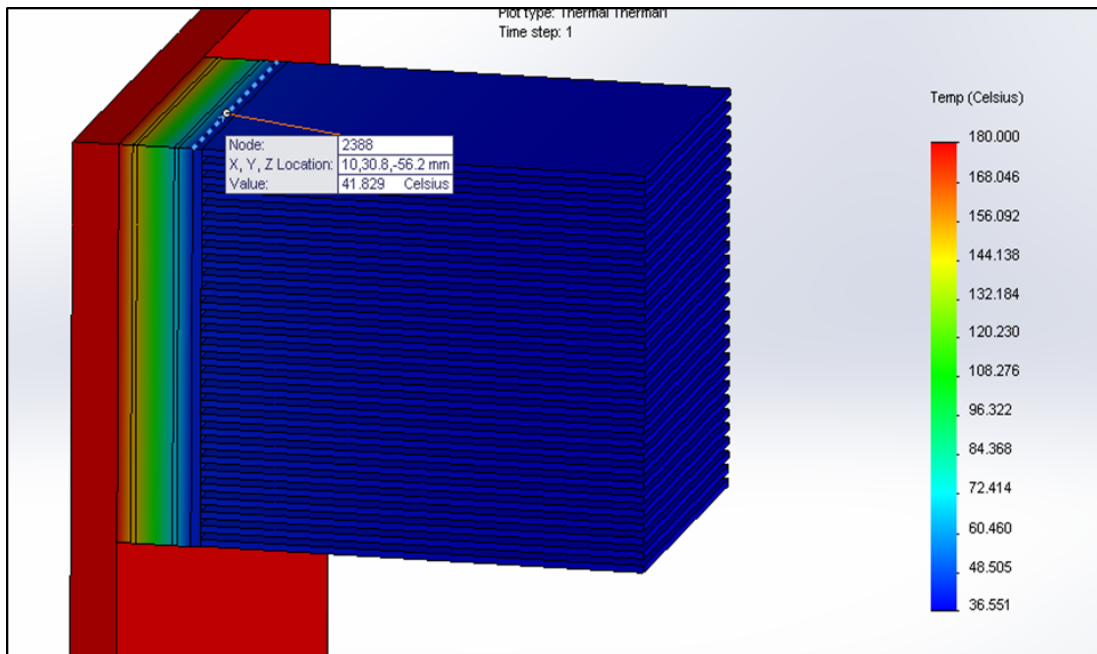


Figure 13. At  $z = 0.7$ mm.

For fin spacing 0.7 mm,  $\Delta T$  came out to be 139 °C as shown in Figure 13.

Situation 4: Fin thickness = 0.6 mm and Fin height = 44.40 mm

At  $z = 0.5$  mm

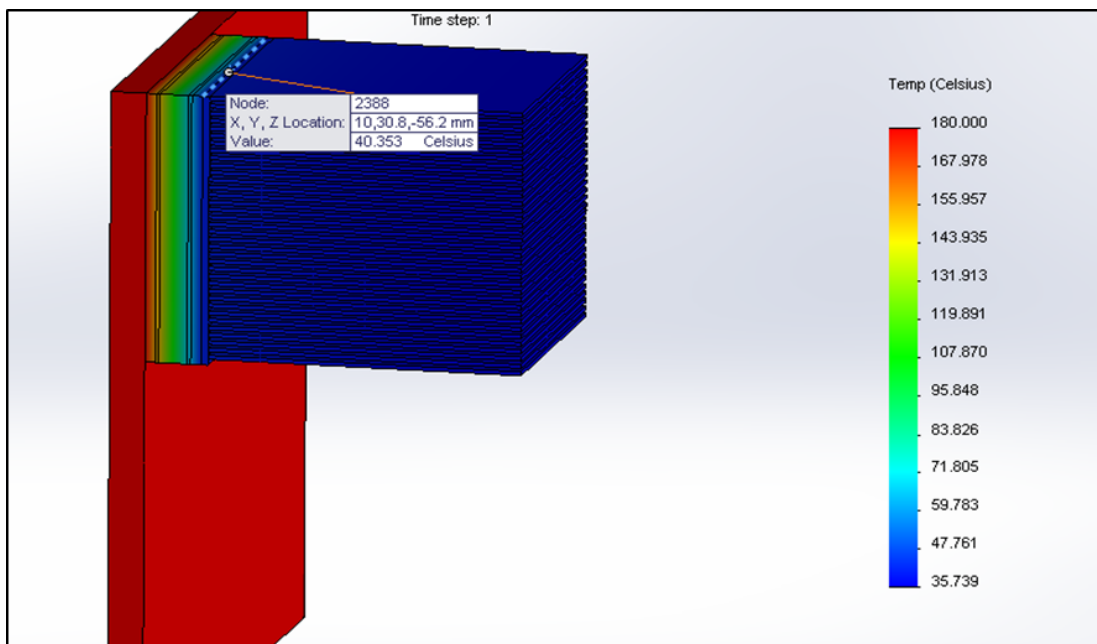
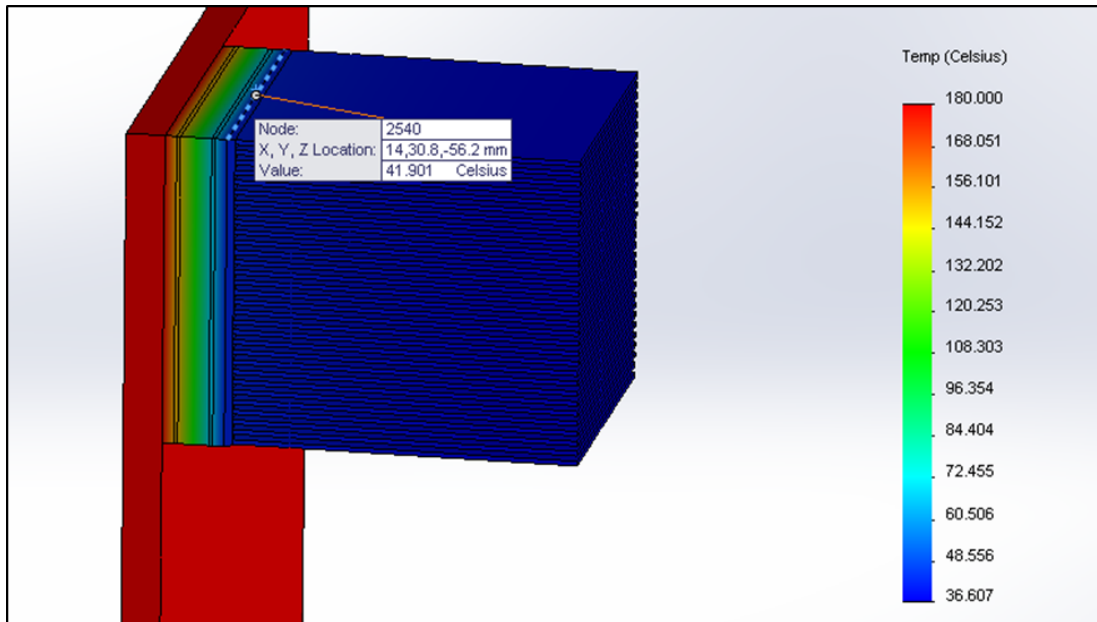


Figure 14. At  $z = 0.5$ mm.

For fin spacing of 0.5 mm,  $\Delta T$  came out to be 140 °C as shown in Figure 14.  
At  $z = 0.7$  mm



**Figure 15.** At  $z = 0.7$ mm.

For fin spacing of 0.7 mm,  $\Delta T$  came out to be 132 °C as shown in Figure 15.  
At  $z = 0.9$  mm

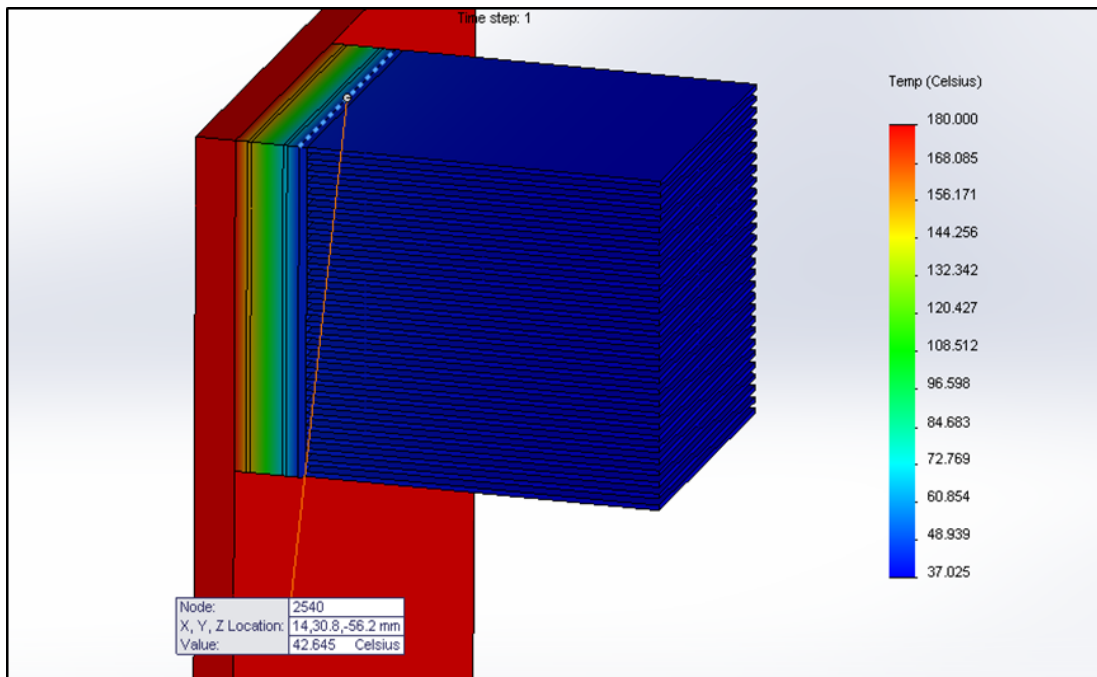


**Figure 16.** At  $z = 0.9$ mm.

For fin spacing of 0.9 mm,  $\Delta T$  came out to be 137 °C as shown in Figure 16. At  $z = 1.0$  mm

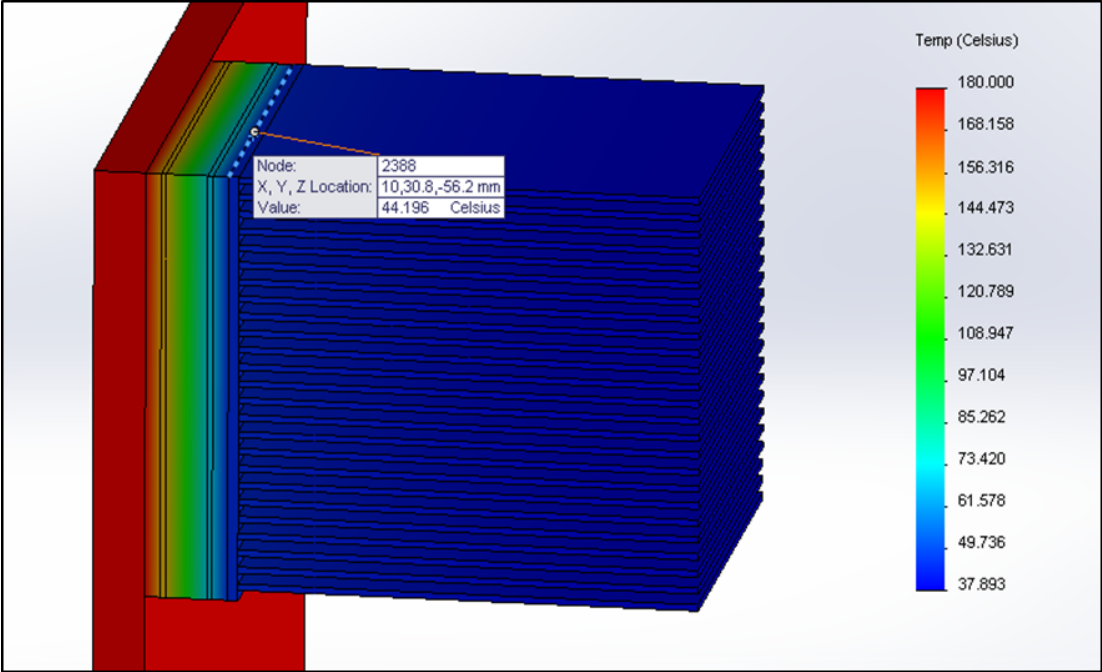


Figure 17. At z = 1mm.

For fin spacing of 1 mm,  $\Delta T$  came out to be 135 °C as shown in Figure 17.

Situation 5: Fin thickness = 0.5 mm and Fin height = 40 mm

At z = 0.5 mm

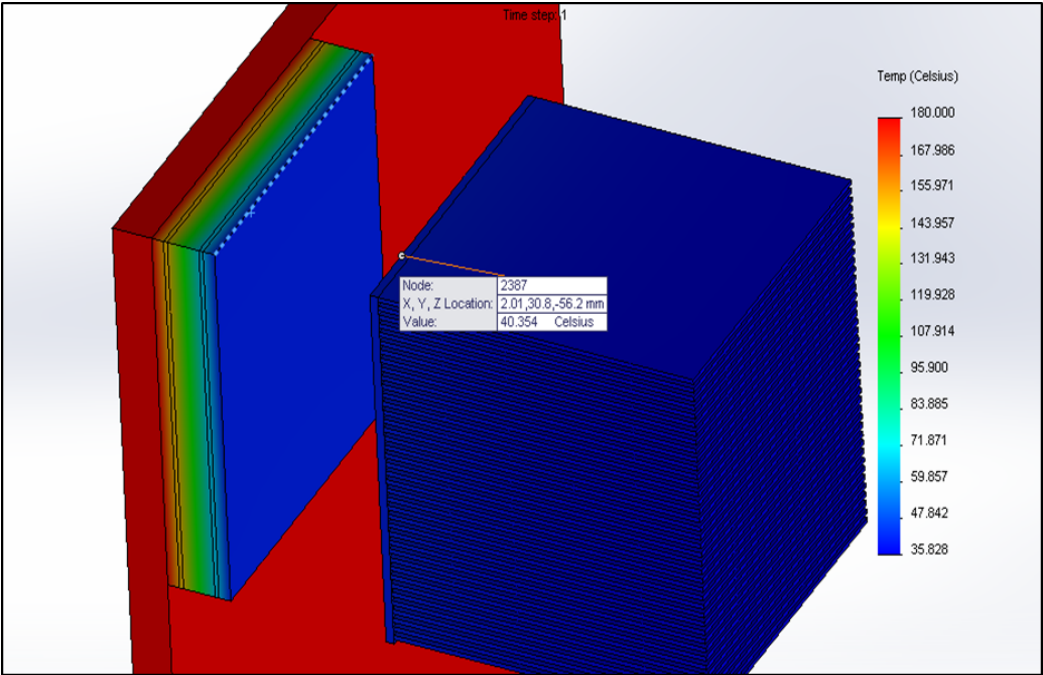


Figure 18. At z = 0.5mm.

For fin spacing of 0.5 mm,  $\Delta T$  came out to be 140 °C as shown in Figure 18.  
At  $z = 0.7$  mm

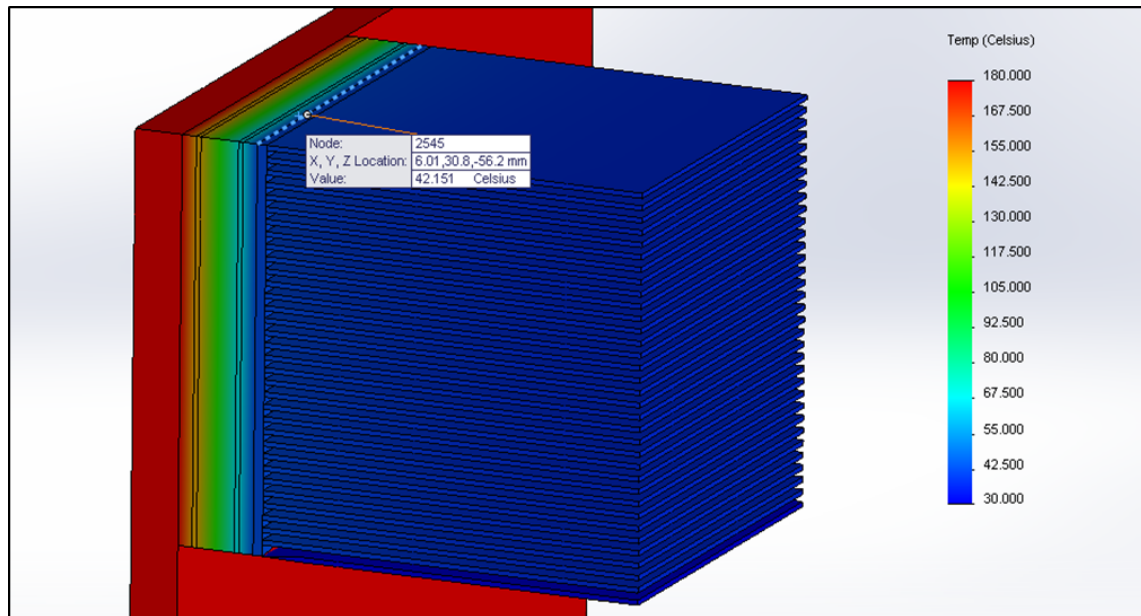


Figure 19. At  $z = 0.7$ mm.

For fin spacing of 0.7 mm,  $\Delta T$  came out to be 132 °C as shown in Figure 19.  
At  $z = 0.9$  mm

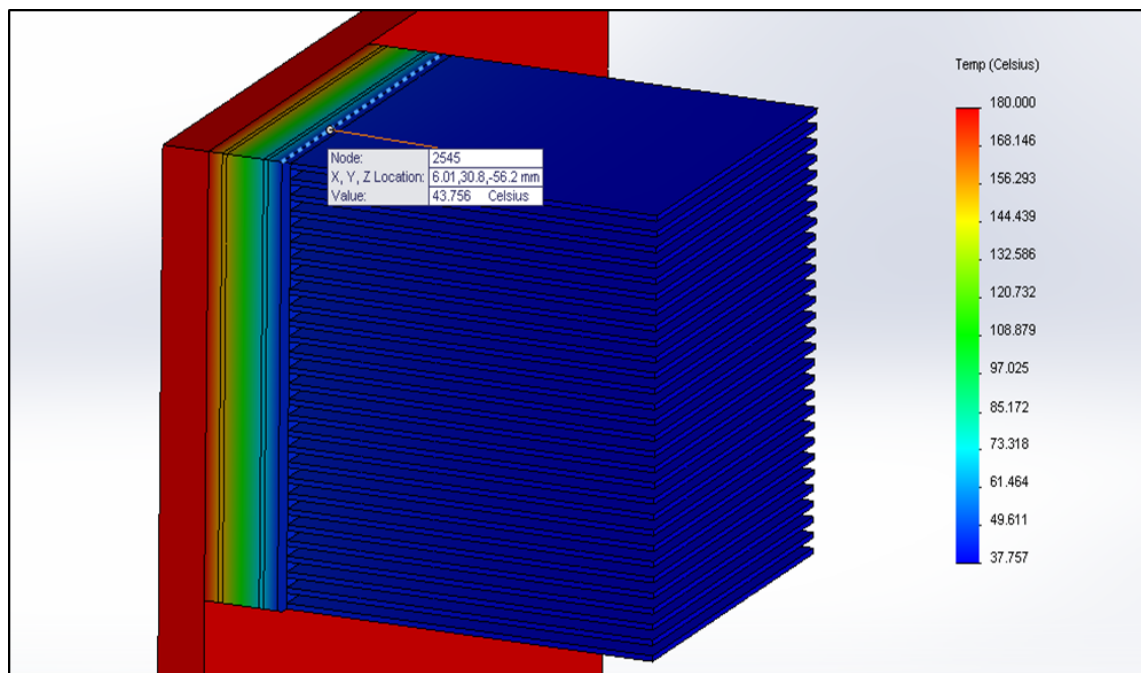


Figure 20. At  $z = 0.92$ mm.

For fin spacing of 0.9 mm,  $\Delta T$  came out to be 136 °C as shown in Figure 20.  
At  $z = 1.0$  mm

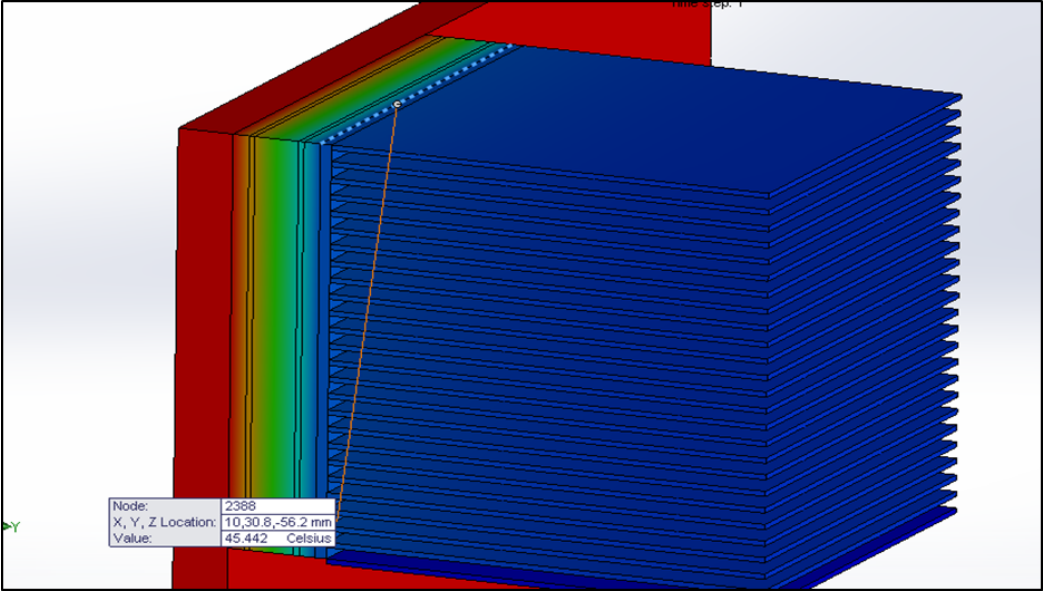


Figure 21. At z = 1mm.

For fin spacing of 1 mm,  $\Delta T$  came out to be 134 °C as shown in Figure 21.  
Situation 6: Tapered Fin with Fin thickness = 0.5 mm and Fin height = 40 mm

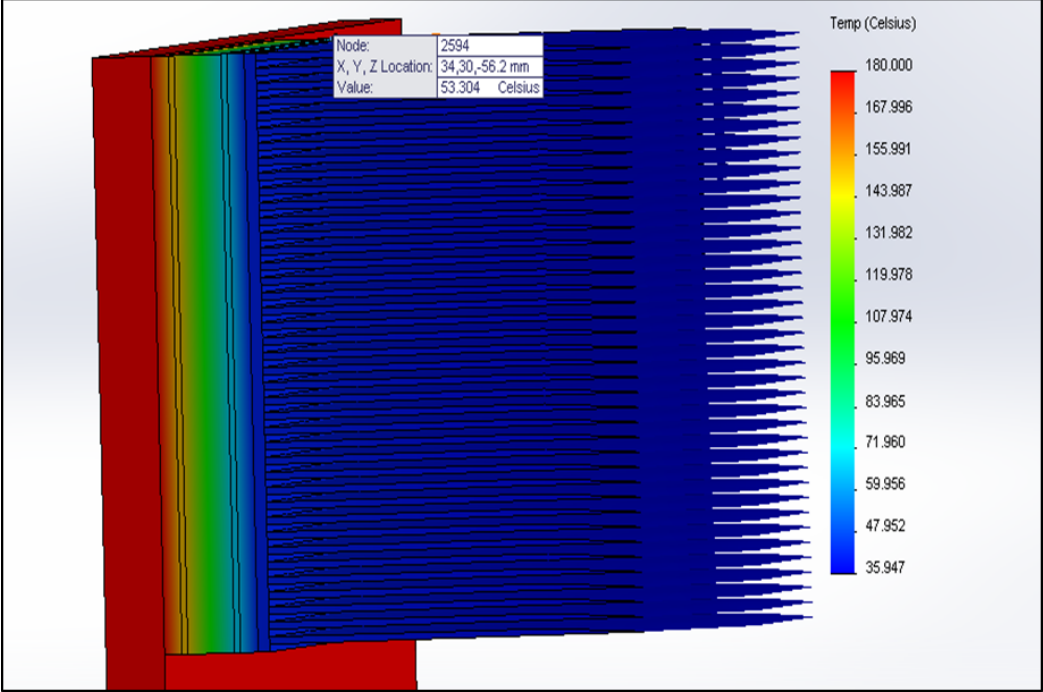


Figure 22. At z = 0.5mm.

For tapered fin with fin spacing of 1 mm, fin thickness of 0.5 mm, and fin height of 40 mm, the  $\Delta T$  came out to be 136 °C, which in the case of uniform thickness fin is 140 °C as shown in Figure 22. Because of this, tapered fins were removed from the consideration for use on TEG.

Keeping in mind the weight, manufacturability, and other constraints for fins, it can be concluded that a temperature difference of 140 °C can be achieved between the hot and cold side of the thermoelectric generator by using a rectangular fin heat sink of the following specifications:

- Base plate length = 40 mm.
- Base plate width = 40 mm.
- Base plate thickness = 1 mm.
- Fin thickness = 0.5 mm.
- Fin height = 40 mm.
- Fin spacing = 0.5 mm.

## 5. Experiment Setup

In addition to numerical analysis, an experimental investigation has been carried out by using a prototype power plant having similar working conditions to the powerplant in PPCL, Karaikal, India. The preliminary aim of the analysis is to construct an indoor prototype of powerplant conditions in Pondicherry Power Corporation Limited (PPCL) located at Karaikal and find the power output of the commercial thermoelectric generator at the constructed operating condition. Further, a study is analyzed to obtain the correlation between various parameters. The equipment used for constructing the prototype powerplant is as follows:

- Thermoelectric generator,
- Anemometer,
- Thermocouple,
- Burner,
- Stand,
- Fins,
- Pedestal fan,
- Multimeter,
- Metal sheet,
- Thermal grease,
- Connecting wires.

An LPG cylinder (2 liters) was used as the burner. Two K-type thermocouples were employed for temperature measurement. Three multi-meters were used to measure the temperature and voltage generated from TEG. Aluminum sheets were used as metal sheets. A pedestal fan was used to generate wind with the required wind speed and to simulate a forced convection analysis in the indoor environment. An anemometer was used to measure the wind speed. The schematic of the experimental test rig is shown in Figure 23.

In the analysis of the experimental system, the investigation of uncertainties in measured quantities is crucial for achieving accurate results. Errors in this context are classified into two primary categories: random errors and systematic errors. Given the specific conditions of the study, systematic errors are not present. Therefore, the focus is on random errors, which can be quantified through statistical methods and directly derived from the data provided by the measuring instruments. Random errors, being inherently unpredictable and varying with each measurement, require thorough statistical analysis to understand their impact on the overall results and to ensure the reliability of the findings.

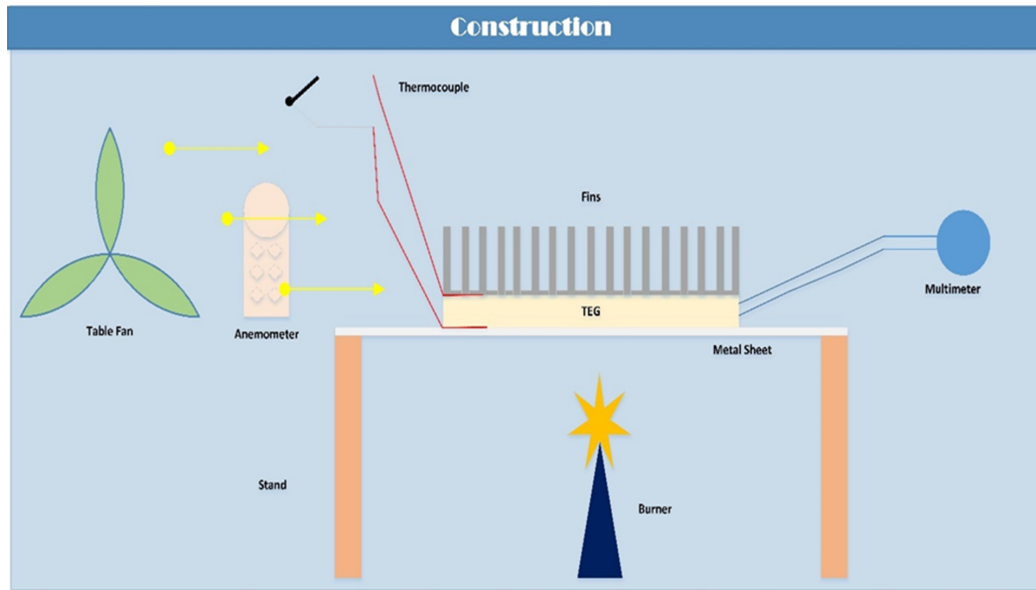


**Figure 23.** Schematic of the experimental setup.

The uncertainties in measuring instruments are estimated using the following relation [37–39]:

$$w_r = \left[ \left( \frac{\partial R}{\partial x_1} w_1 \right)^2 + \left( \frac{\partial R}{\partial x_2} w_2 \right)^2 + \dots + \left( \frac{\partial R}{\partial x_n} w_n \right)^2 \right]^{1/2}. \quad (1)$$

In the analysis of the system, the anticipated margin was initially estimated at 1%. This estimate considered potential inaccuracies inherent to the measuring instruments employed. A meticulous examination of the daily output revealed that the variations in the measurements fell within a more refined range of  $\pm 0.5\%$ .

Furthermore, the study addressed the potential errors related to the measurement of temperature and electrical power, which were quantified at 0.1% and 0.05%, respectively. Incorporating these factors into the overall assessment, the cumulative imprecision in evaluating the efficiency of the system was projected to be approximately  $\pm 2\%$ . This comprehensive error margin underscores the reliability of the solar drying system while acknowledging the inevitable limitations in measurement precision.

### 5.1. Experimental Procedure

The TEG is attached to the metal sheets with the use of thermal grease. The metal sheet plays the role of a chimney wall. The metal sheet is supported by a stand. The pedestal fan is used to simulate the required wind speed (forced convection). The metal sheet surface is exposed to the flames of the burner and gets heated to reach a steady-state temperature of  $45^\circ\text{C}$ . The thermocouple is used to record the temperatures of  $T_h$  and  $T_c$ . The TEG output terminals are connected to a multimeter to read the output voltage and current. The output voltage (mV) is measured after the setup reaches a steady temperature. The temperature is now increased in steps of  $15^\circ\text{C}$  from  $50^\circ\text{C}$  to  $150^\circ\text{C}$  and the corresponding output voltage is measured. The output data obtained is used to develop a correlation. The experimental setup with and without fins is shown in Figures 24 and 25.

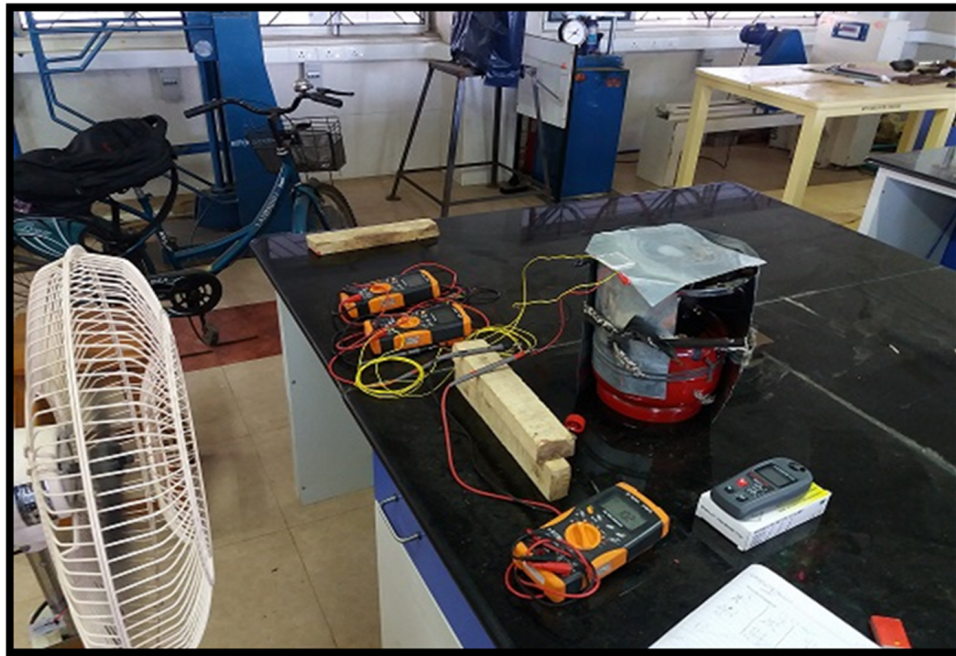


**Figure 24.** Experimental Setup without fins (forced convection).



**Figure 25.** Experimental Setup with fins (forced convection).

## 6. Results

The experimental results based on the various configurations have been discussed in the following subsections. The experimental conditions with different wind velocities and the respective results are shown in Figures 26 to 30.

### 6.1. Forced convection without fins at a velocity of 3.3 m/s

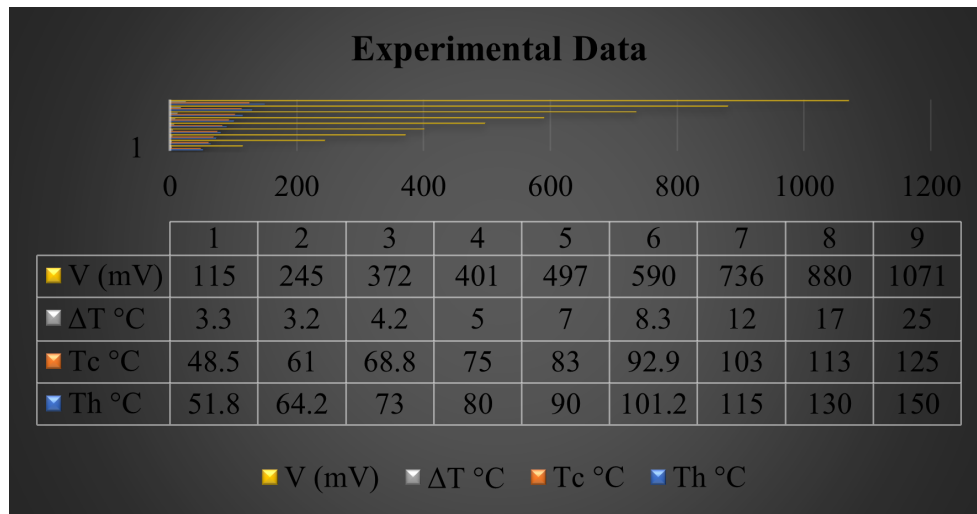


Figure 26. Experimental data for forced convection without fins at velocity 3.3 m/s.

### 6.2. Forced convection without fins at a velocity of 4 m/s

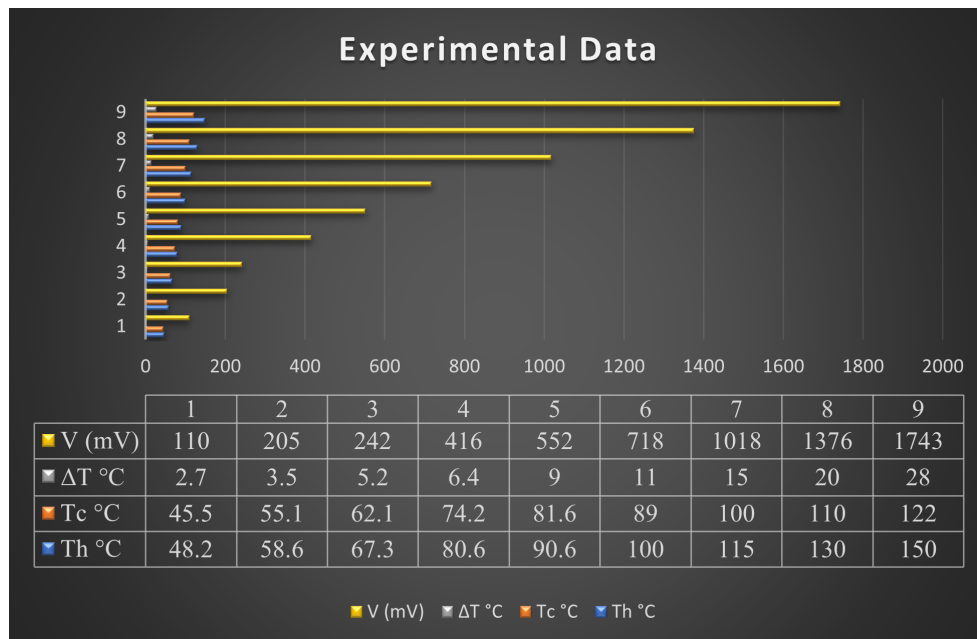


Figure 27. Experimental data for forced convection without fins at velocity 4 m/s.

6.3. Forced convection without fins at a velocity of 4.4 m/s

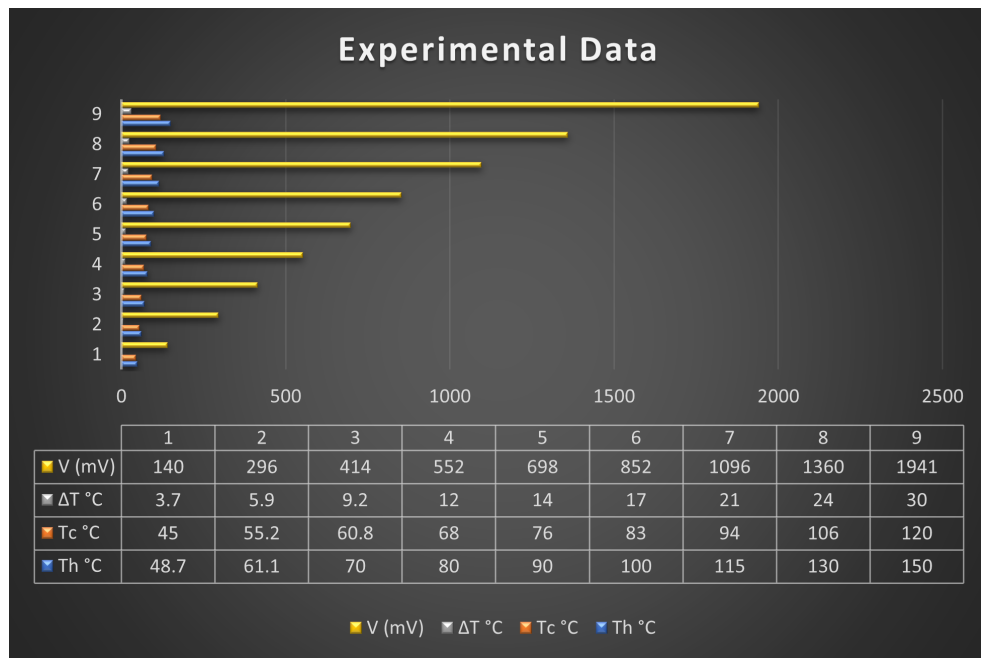


Figure 28. Experimental data for forced convection without fins at velocity 4.4 m/s.

6.4. Forced convection with fins at a velocity of 2.8 m/s

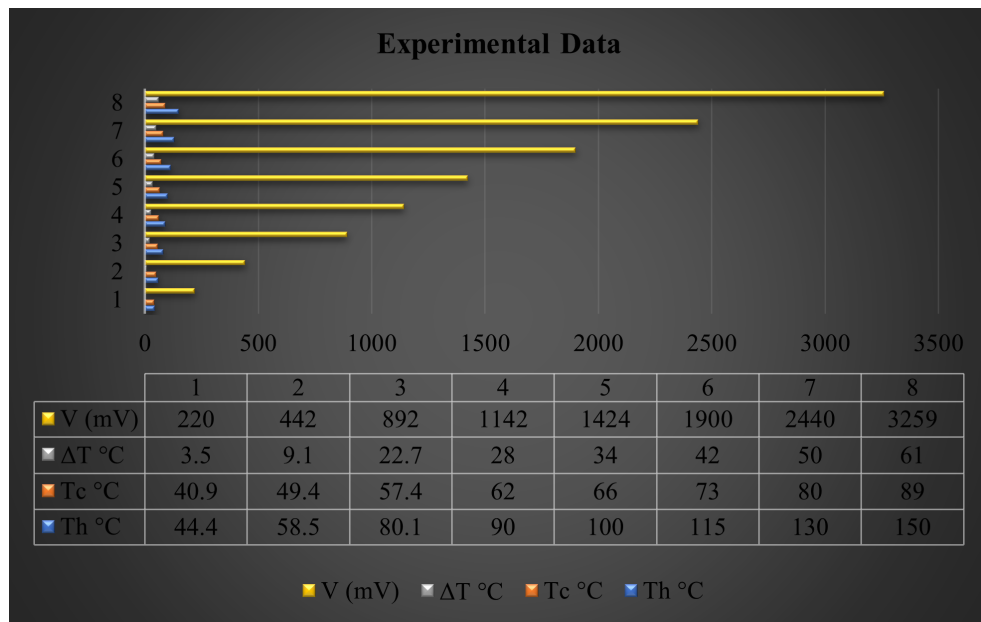


Figure 29. Experimental data for forced convection with fins at velocity 2.8 m/s.

6.5. Forced convection with fins at a velocity of 3.1 m/s

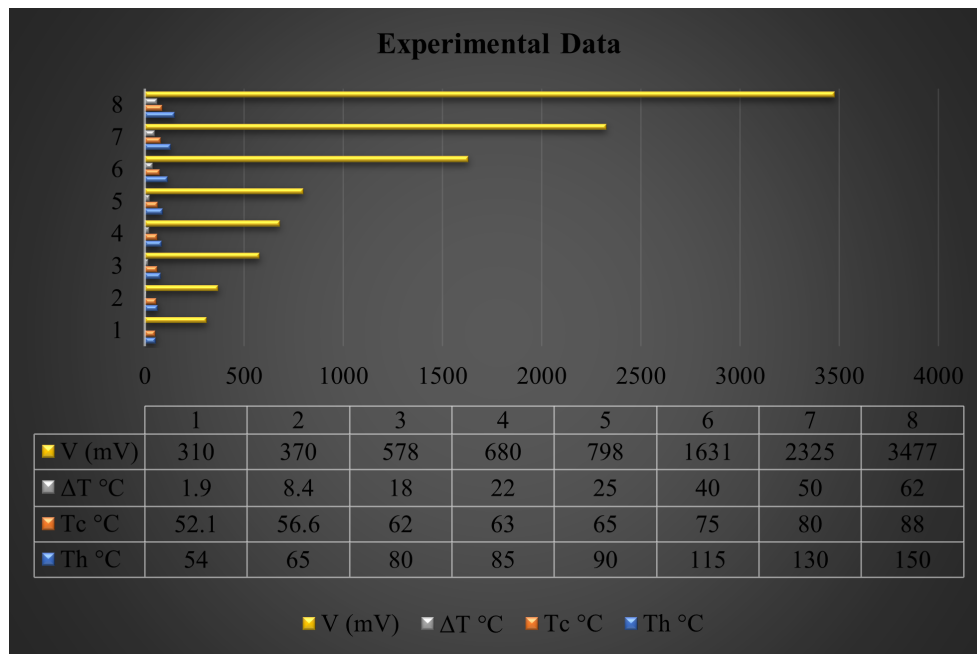


Figure 30. Forced Convection without fins at a velocity of 3.3 m/s.

6.6. Variation of cold plate temperature for hot plate temperature

The variation of cold plate temperature according to hot plate temperature with different wind velocities and the respective results are shown in Figures 31 to 35.

6.6.1. Forced Convection without fins at a velocity of 3.3 m/s

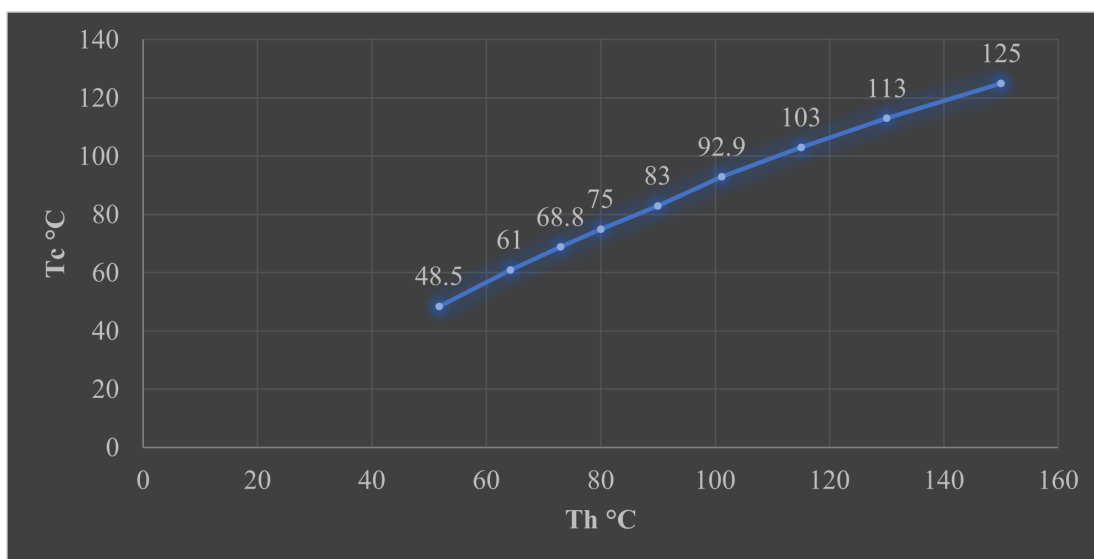
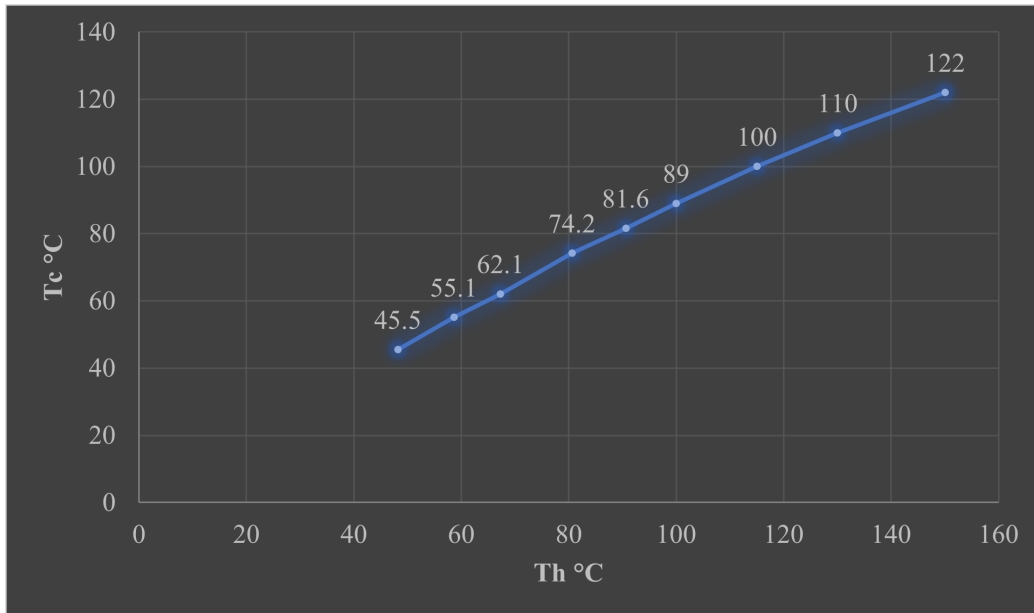


Figure 31. Variation of T<sub>c</sub> Vs T<sub>h</sub> for forced convection without fins at velocity 3.3 m/s.

At a velocity of 3.3 m/s and hot plate temperature 150 °C, cold plate temperature was obtained to be 125 °C as shown in Figure 31.

6.6.2. Forced Convection without fins at a velocity of 4 m/s



**Figure 32.** Variation of  $T_c$  Vs  $T_h$  for forced convection without fins at velocity 4 m/s.

At a velocity of 4 m/s and hot plate temperature 150 °C, cold plate temperature was obtained to be 122 °C as shown in Figure 32.

6.6.3. Forced convection without fins at a velocity of 4.4 m/s

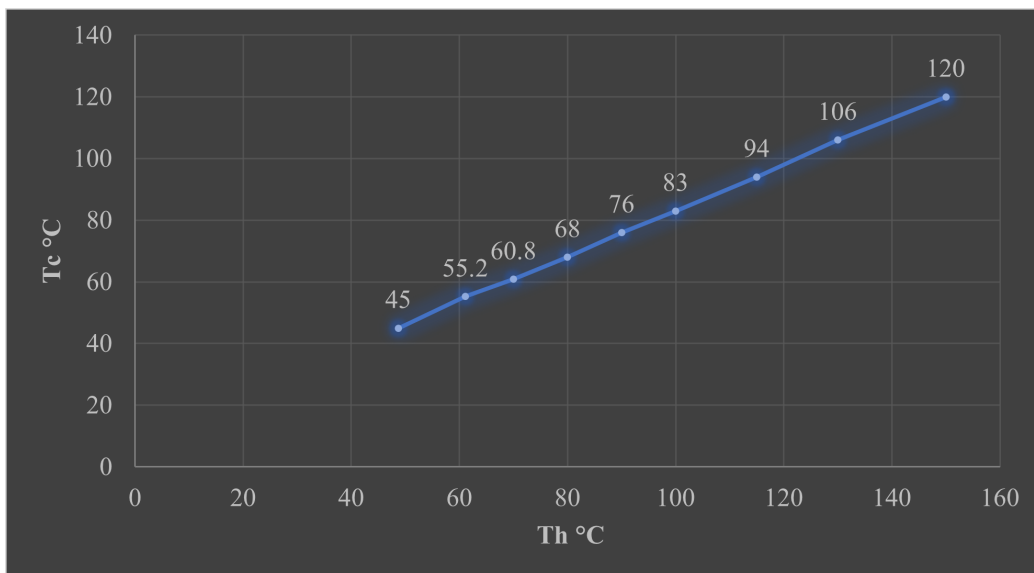


**Figure 33.** Variation of  $T_c$  Vs  $T_h$  for forced convection without fins at velocity 4.4 m/s.

At a velocity of 4.4 m/s and hot plate temperature of 150 °C, the cold plate temperature was obtained to be 120 °C as shown in Figure 33.

6.6.4. Forced Convection with fins at a velocity of 2.8 m/s

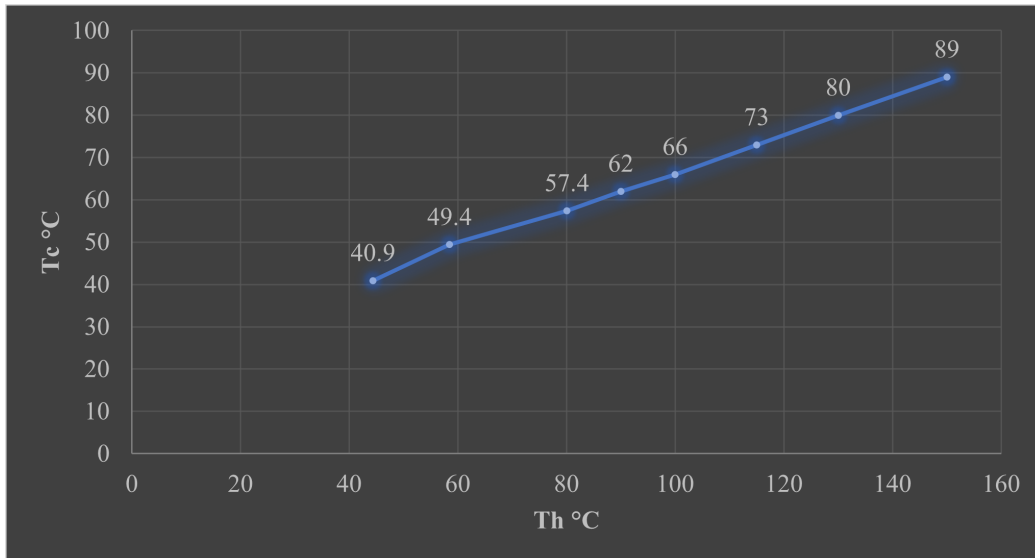


**Figure 34.** Variation of  $T_c$  Vs  $T_h$  for forced convection with fins at velocity 2.8 m/s.

At a velocity of 2.8 m/s and hot plate temperature 150 °C, cold plate temperature was obtained to be 89 °C which is way lesser than what was obtained without fin on the TEG as shown in Figure 34.

6.6.5. Forced Convection with fins at a velocity of 3.1 m/s

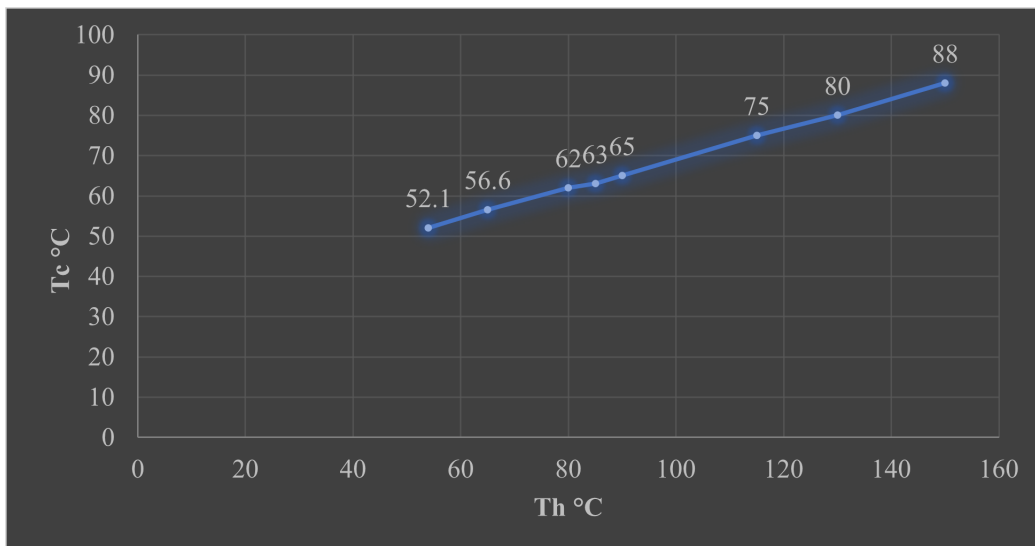


**Figure 35.** Variation of  $T_c$  Vs  $T_h$  for forced convection with fins at velocity 3.1 m/s.

At a velocity of 3.1 m/s and hot plate temperature 150 °C, cold plate temperature was obtained to be 88 °C as shown in Figure 35.

6.7. EMF Produced for varying Temperature Difference

The variation of EMF generation according to varying temperatures with different wind velocities is shown in Figures 36 to 40.

6.7.1. Forced Convection without fins at a Velocity of 3.3 m/s

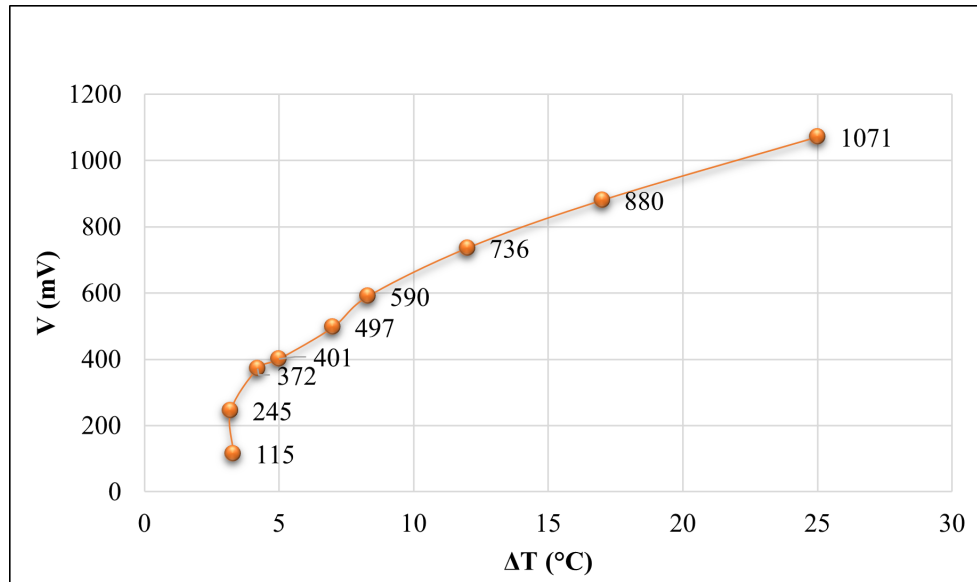


Figure 36. EMF produced for  $\Delta T$  without fins at velocity 3.3 m/s.

For a temperature difference of 25°C, the EMF produced was 1071 mV as shown in Figure 36.

6.7.2. Forced Convection without Fins at a Velocity of 4 m/s

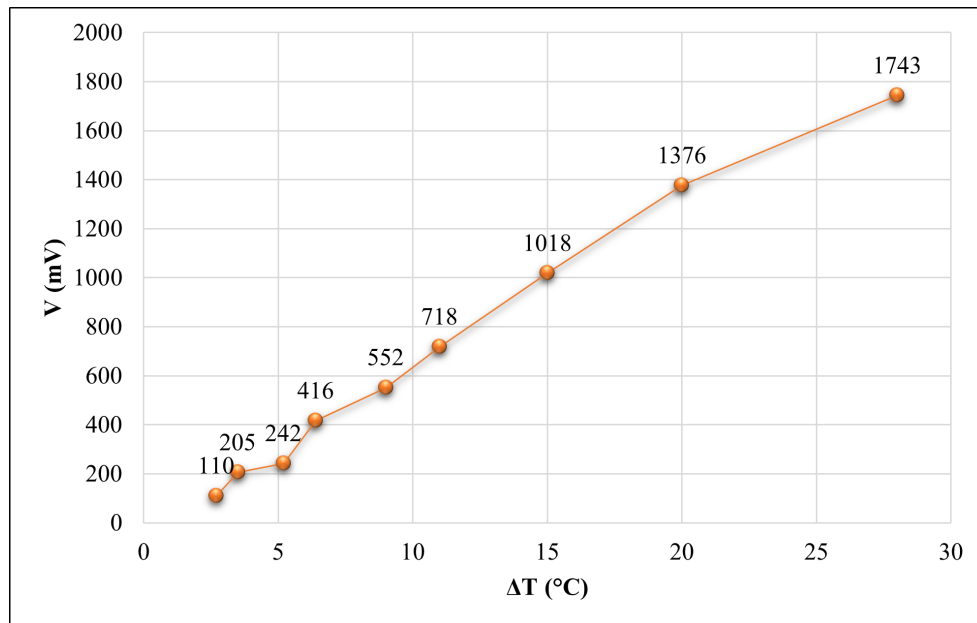


Figure 37. EMF produced for  $\Delta T$  without fins at velocity 4 m/s.

For a temperature difference of 27°C, the EMF produced was 1743 mV as shown in Figure 37.

6.7.3. Forced Convection without Fins at a Velocity of 4.4 m/s

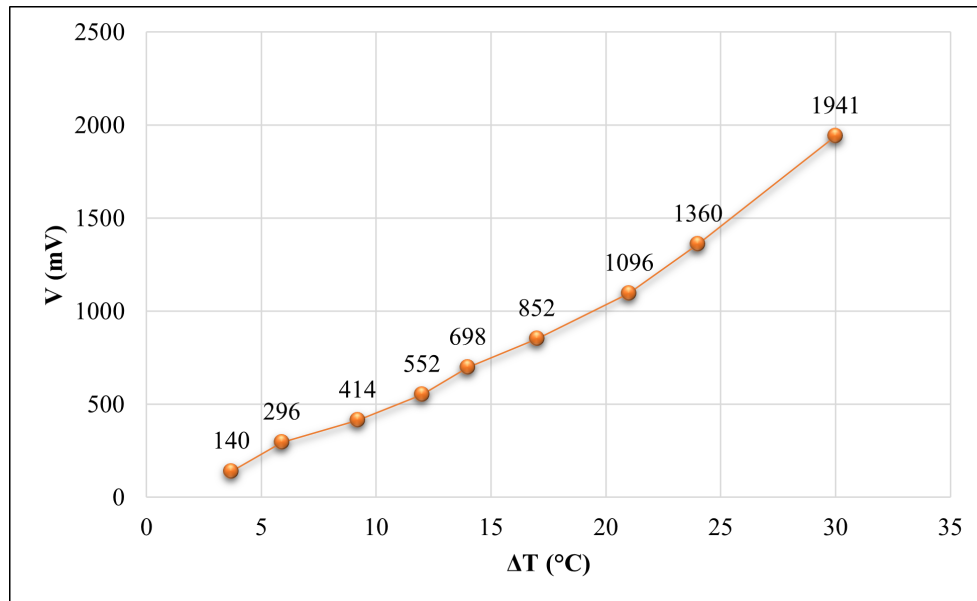


Figure 38. EMF produced for  $\Delta T$  without fins at velocity 4.4 m/s.

For a temperature difference of 30°C, the EMF produced was 1941 mV as shown in Figure 38.

6.7.4. Forced Convection with Fins at a Velocity of 2.8 m/s

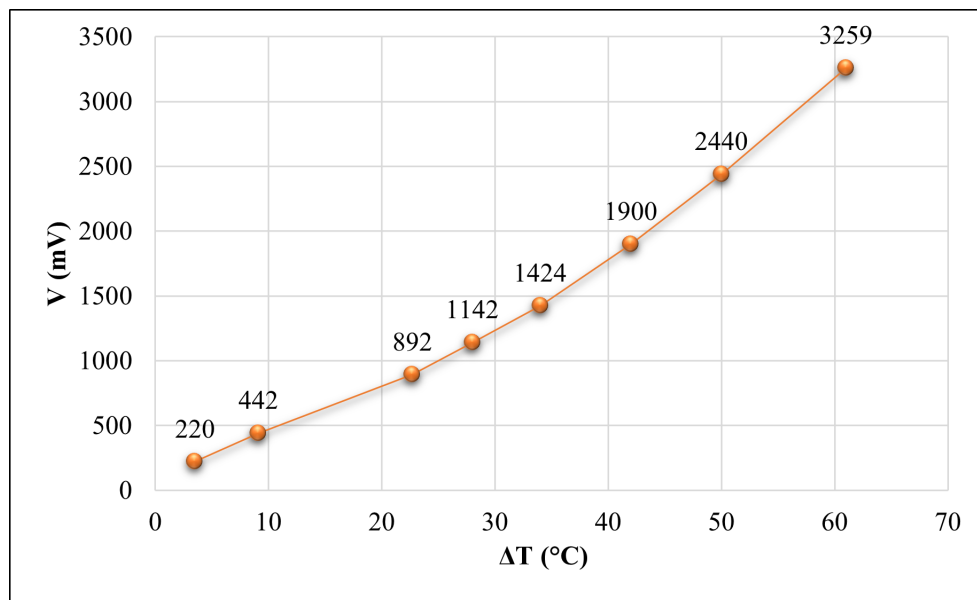
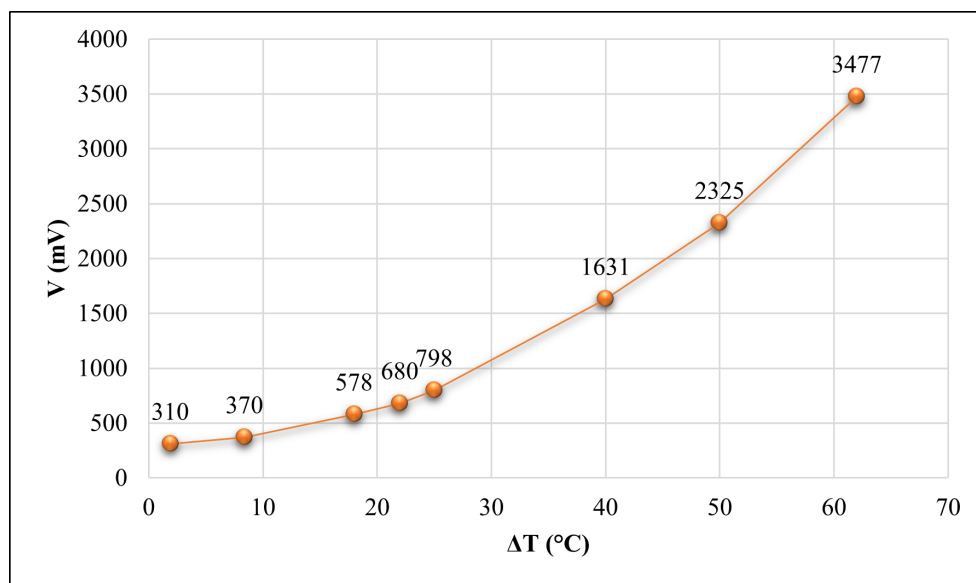


Figure 39. EMF produced for  $\Delta T$  without fins at velocity 2.8 m/s.

For a temperature difference of 60°C, the EMF produced was 3259 mV as shown in Figure 39.

6.7.5. Forced Convection with Fins at Velocity 3.1 m/s



**Figure 40.** EMF produced for  $\Delta T$  without fins at velocity 3.1 m/s.

For a temperature difference of 62°C, the EMF produced was 3477 mV as shown in Figure 40. The results were obtained for the various cases of forced convection at various velocities of 4.4 m/s, 4 m/s, 3.3 m/s without fins, and velocities of 2.8 m/s and 3.1 m/s with fins. Also, variation of cold plate temperature for hot plate temperature EMF produced for varying temperature differences is plotted.

*Thermal Gradients and Electrical Outputs*

To strengthen the findings of this study, specific data on the thermal gradients and corresponding electrical outputs under varying operating conditions have been incorporated. Table 2 summarizes the observed thermal gradients ( $\Delta T$ ) along with the electrical outputs ( $V$ ) for different hot plate temperatures ( $T_h$ ) at various wind velocities.

**Table 2.** Thermal Gradients and Electrical Outputs under Different Operating Conditions.

$T_h$ (°C)	$\Delta T$ (°C)	V (mV) at Velocity 2.8 m/s	V (mV) at Velocity 3.1 m/s
50	3.3	115	310
100	9.1	590	1631
150	25	1071	3477

The data indicates that as the thermal gradient increases, the electrical output generated by the TEGs also rises. For instance, at a hot plate temperature of 150 °C, a thermal gradient of 25 °C yielded an output of 1071 mV at a wind velocity of 2.8 m/s, while the same condition at 3.1 m/s produced an output of 3477 mV. This correlation not only reinforces the findings of the experimental validation but also underscores the effectiveness of TEGs in harnessing waste heat energy for power generation.

Furthermore, the results presented in this study were validated through a combination of numerical simulations and experimental investigations. The numerical analysis involved detailed parametric simulations, where different configurations of the Thermoelectric Generators (TEGs) were assessed under varying thermal and physical conditions to ensure accuracy in predictions. The parameters were

carefully selected based on real-world conditions observed at the power plant. These simulated results were then validated by constructing a prototype replicating the operational environment of the power plant in Pondicherry Power Corporation Limited (PPCL). The consistency between the numerical and experimental results confirms the accuracy and robustness of the findings.

Furthermore, standard procedures were followed to ensure that the measurement errors were minimized, and multiple trials were conducted to reinforce the repeatability of the results. Through this prototype, experimental data were gathered, and key parameters such as temperature difference ( $\Delta T$ ), wind velocities, and electrical power output were meticulously measured and compared against the simulated values. The strong agreement between the numerical and experimental findings affirms the reliability of the results presented. Additionally, careful consideration was given to the practical conditions under which the TEGs were implemented, ensuring real-world applicability and the robustness of the validation process. The close alignment between both data sets demonstrates the effectiveness of the chosen methods in predicting the behavior of Thermoelectric Generators (TEGs) in waste heat recovery.

## 7. Recommendations to PPCL powerplant for deploying TEGs to produce electricity from waste heat

### 7.1. Proposed Thermoelectric Generator Specifications and Characteristics

A commercially available TEG (TEG1-PB-12611-6.0) is chosen and the specifications and characteristics of TEG are shown in Figures 41 and 42.

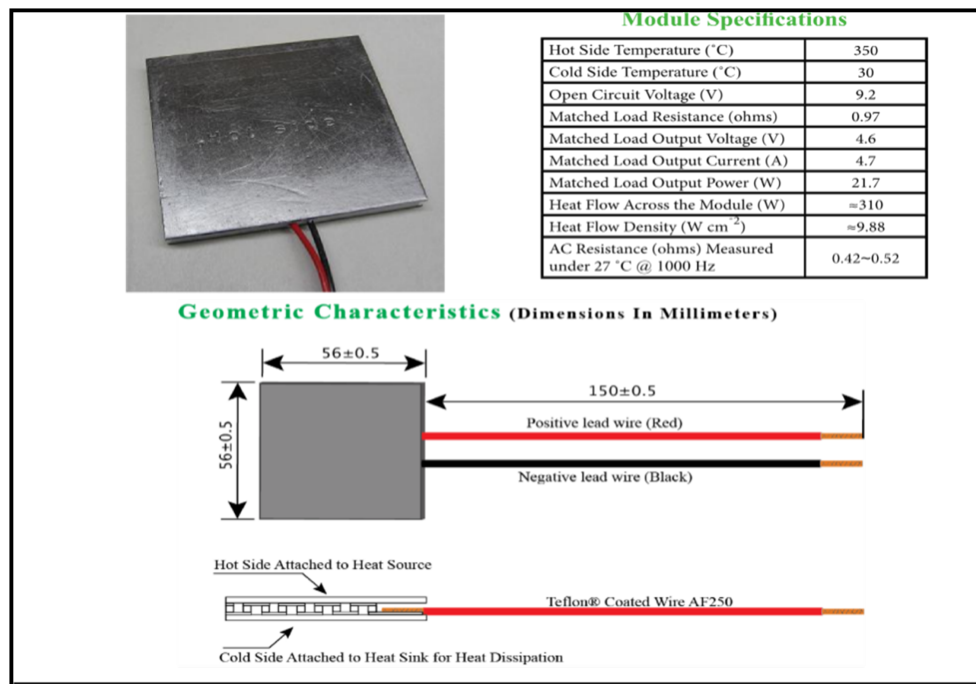


**Figure 41.** TEG1-PB-12611-6.0 Specifications Courtesy: (www.tecteg.com).

#### 7.1.1. Selection of Thermoelectric Materials

The selection of thermoelectric materials is critical to the performance and efficiency of Thermoelectric Generators (TEGs). This study primarily focuses on Bismuth Telluride (Bi<sub>2</sub>Te<sub>3</sub>), which has long been the benchmark material in thermoelectric applications due to its advantageous properties. Bi<sub>2</sub>Te<sub>3</sub> exhibits a

high Seebeck coefficient (approximately  $200 \mu\text{V/K}$  at room temperature), favorable electrical conductivity, and relatively low thermal conductivity, facilitating efficient energy conversion in TEGs. However, the material's effectiveness is constrained by its operational temperature limit of around  $300 \text{ }^\circ\text{C}$ , which poses challenges in high-temperature applications. Thus, alternative materials, such as Silicon-Germanium (SiGe), Skutterudites, and Oxides, are being investigated for their high-temperature performance and stability. These materials often present a trade-off between efficiency and operational range; for example, while SiGe can operate at temperatures exceeding  $800 \text{ }^\circ\text{C}$ , its Seebeck coefficient is significantly lower than that of Bi<sub>2</sub>Te<sub>3</sub>. The performance of TEGs is significantly impacted by these material properties. The Seebeck coefficient directly influences the voltage output generated for a given temperature gradient, while the electrical conductivity affects the current flow. Conversely, the thermal conductivity must be minimized to maintain the temperature difference across the thermoelectric elements, as excessive heat loss to the cold side diminishes overall efficiency. Optimizing the selection of thermoelectric materials based on the intended application is essential for enhancing TEG efficiency. Future research directions may include the exploration of advanced nanostructured materials and composite materials that can potentially overcome the limitations of traditional thermoelectric materials, offering improved performance over a wider range of temperatures.

Additionally, aluminum sheets were selected as the heat-conducting material due to their high thermal conductivity and ease of fabrication, which allows for effective heat transfer between the waste heat source and the thermoelectric generator (TEG). Fins made of aluminum were also incorporated into the design to enhance convective heat transfer and increase the temperature difference across the TEG, thus improving power output. Also, ceramic porcelain was utilized as the substrate material for the thermoelectric modules because of its excellent thermal stability and insulating properties, ensuring safe and reliable operation under high-temperature conditions. The combination of these materials allows for effective temperature differentials across the thermoelectric generator, which is crucial for maximizing energy conversion efficiency.

7.2. Characteristics of TEG1-PB-12611-6.0

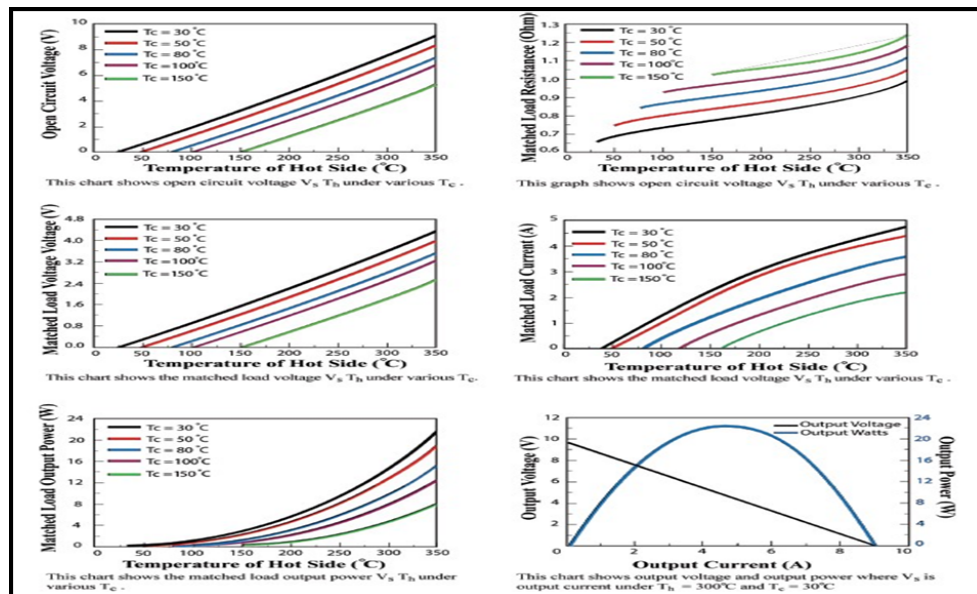


Figure 42. TEG1-PB-12611-6.0 Specifications Courtesy: (www.tecteg.com).

### 7.3. Recommended Thermal Paste

Arctic Silver 5 is selected because of its high-density micronized silver filling and improved thermally conductive ceramic particles. It is a modernized solution for high-power CPUs and high-performance heat sinks. Also, it is made up of 99.9% pure silver. It possesses high density and is electrically nonconductive with greater stability. The range of temperature is about  $-50^{\circ}\text{C}$  to  $180^{\circ}\text{C}$ .

### 7.4. Items recommended for the TEG installation

#### 7.4.1. Thermoelectric generators:

A length of 10 m will be covered by the Thermoelectric Generators on the chimney.

Considering the dimensions of the TEG to be  $56 \times 56 \times 4$  mm and a clearance of 2 cm between each TEG, The total number of TEGs that can be pasted in the whole length of 10 m = 131

Diameter of the chimney = 3 m,

Therefore, the circumference of the chimney =  $2 \times 3.14 \times 1.5 = 9.42$  m

The total number of TEGs that can be pasted on the circumference of the chimney = 123

Therefore, the total number of TEGs which can be pasted on the required area = 16113

#### 7.4.2. Heat sinks:

Since each TEG requires a heat sink, therefore, a total of 16113 heat sinks will also be required.

#### 7.4.3. Thermal paste:

A thermal paste of 5 grams is enough to paste 5 TEGs on the chimney and 5 heat sinks on 5 TEGs. Therefore, for pasting 16113 TEGs on the chimney and heat sinks on them, a total of 16113 grams or 16.113 kg of thermal paste will be required.

#### 7.4.4. Maximum power point trackers

Due to changing weather conditions, there will be a fluctuation in the cold plate temperature of the TEG which can cause a fluctuation in power delivered and a change in the characteristics curve. Therefore, it is highly recommended to employ MPPT to track the maximum power point and extract the maximum power out of the TEG in a given situation.

#### 7.4.5. The power produced by the TEGs:

The wall of the chimney is always at a constant temperature of  $180^{\circ}\text{C}$  when the plant is working at 100% capacity, and from the experimental data, we know that the cold side plate temperature of the TEG will be  $70^{\circ}\text{C}$ . From the graph of matched load output power vs hot plate temperature, we can say that the power produced by one TEG will be equal to 3.8 watts.

Therefore, power produced by all the TEGs =  $16113 \times 3.8 = 61$  kW

Total power delivered by the TEGs = Power produced by the TEGs  $\times$  MPPT efficiency  $\times$  Inverter efficiency =  $61 \times 0.95 \times 0.95 = 55$  kW

#### 7.4.6. Selection of MPPT:

Since the voltage supply is to be 240 V, a 10 kW/240 V solar charge controller will be a good choice, and as the power produced by the TEGs is 61 kW, therefore, a total of 7 MPPTs will be required for the project.

#### 7.4.7. Inverter:

Since the power produced by the TEGs is 61 kW, therefore, a standard 70 kVA inverter will be perfect for the project.

#### 7.5. Integration of TEGs with HRSG System

The integration of Thermo-Electric Generators (TEGs) with the Heat Recovery Steam Generator (HRSG) system is a pivotal aspect of this study. This section outlines the integration process in detail, complemented by schematics for clarity.

##### 1. System Overview:

The TEGs are positioned on the chimney wall of the HRSG, where they exploit the waste heat emitted during the steam generation process. The design ensures optimal thermal contact between the TEGs and the chimney surface.

##### 2. Step-by-Step Integration Process:

- **Preparation:** Ensure that the chimney surface is free from any insulation in the area where the TEGs will be affixed. This is critical for maximizing thermal conduction.
- **TEG Installation:** Apply a suitable thermal paste to the TEG base to enhance heat transfer. Secure the TEGs onto the chimney wall, ensuring a snug fit to eliminate air pockets that could impede thermal conductivity.
- **Connection to Electrical System:** Connect the TEG output terminals to the power management system, ensuring proper electrical connections to facilitate efficient energy harvesting.
- **Monitoring Setup:** Install thermocouples on both the hot and cold sides of the TEGs to monitor temperature differentials. This data is essential for assessing TEG performance and optimizing operational parameters.

##### 3. Operational Considerations:

Maintain the operational integrity of the HRSG and monitor the TEGs to ensure consistent thermal input without excessive disturbances. The power generation findings suggest that while the initial investment may be substantial, the long-term gains are significant.

#### 7.6. Economic Analysis

##### 7.6.1. Cost of Equipment Required

Cost of one TEG = Rs 3000

Therefore, the cost of all TEGs required for the project =  $3000 \times 16113 = \text{Rs } 48,339,000$

The cost of one Heat Sink = Rs 120

Therefore, the cost of all heat sinks required for the project =  $120 \times 16113 = \text{Rs } 1,933,560$

#### Comparative Analysis with Alternative Technologies

1. **Thermoelectric Generators (TEGs):** TEGs are solid-state devices that convert heat directly into electricity using the Seebeck effect. They are reliable, require minimal maintenance, and have no moving parts. However, they generally exhibit lower efficiencies compared to other systems, often ranging between 3% to 8%.

2. **Organic Rankine Cycle (ORC):** ORC systems utilize organic fluids to recover waste heat, converting it into mechanical energy, which is then transformed into electricity through a turbine. ORC systems can achieve efficiencies of up to 15% to 20%, making them more suitable for higher-temperature waste heat sources. However, they entail higher initial costs and require more maintenance compared to TEGs.
3. **Conventional Heat Exchangers:** While heat exchangers effectively transfer heat from a hot fluid to a cooler fluid, they do not generate electricity. Their primary function is to enhance the thermal efficiency of existing systems, which may indirectly lead to energy savings. Unlike TEGs, they do not convert heat into usable electrical energy, thus lacking in direct applicability for power generation.

This comparative examination reveals that while TEGs may not match the efficiency levels of ORC systems, their distinct advantages in specific applications make them a valuable asset in waste heat recovery initiatives. The deployment of TEGs can significantly enhance energy capture in scenarios where traditional systems may be impractical or cost-prohibitive, thereby supporting the overarching goal of improving energy efficiency in various sectors.

### 7.7. Summary

1. **Optimum TEG Thickness:** The study identified an optimum thickness of 8 mm for TEGs, with configurations utilizing fins demonstrating enhanced thermal performance, achieving a temperature difference ( $\Delta T$ ) of up to 110 °C.
2. **Power Generation Efficiency:** Experimental results showed that TEGs with fins produced a maximum power output of 3.8 watts per module at peak operational conditions. The deployment of 16,113 TEGs could yield an estimated total power output of 61 kW under ideal circumstances.
3. **Economic Viability:** An economic analysis revealed a payback period of approximately 24 years for the investment in TEG deployment, underscoring the long-term financial implications of this technology in waste heat recovery.

In conclusion, the study convincingly illustrates the efficacy of TEGs in harnessing waste heat for electric power generation within the specified power plant context. The findings advocate for the strategic deployment of TEGs, highlighting both their operational advantages and economic feasibility in enhancing energy recovery systems.

## 8. Conclusions

The effect of Thermoelectric Generators (TEGs) on electric power generation using waste heat recovery is analyzed numerically and experimentally. Therefore, the 32.5 MW combined cycle power plant located in Karaikal is chosen for this study. The conclusions of the study are as follows:

- Numerical analysis was carried out to find the optimum thickness of TEGs to be installed for electric power generation.
- It was observed that the optimum thickness of TEG with and without fins that were attached to the walls of the chimney for waste heat recovery was 8 mm.
- It is observed that the TEG with fins attached to the cold side has better output.
- A program was formulated to calculate the power generation for various temperature differences ( $\Delta T$ ).
- Further, based on the numerical results, the prototype of a power plant was developed and the effect of TEGs with and without fins at different wind velocities was analyzed. It was observed that the TEG with fins attached to the cold side has better output similar to numerical analysis.

- It was apparent that the experimental results were in good agreement with the numerical results.
- The economic analysis of the deployment of TEGs in a powerplant at PPCL, Karaikal, India for electric power generation was carried out to evaluate the viability. It was observed that the payback period was about 24 years.
- Combining all the obtained results, the TEG with some specific configurations were proposed for PPCL, Karaikal for electricity generation by using waste heat from the combined cycle powerplant.

In summary, the study's results demonstrate significant potential for improving energy efficiency and reducing operational costs through the integration of Thermo-Electric Generators (TEGs) in existing power plants. By effectively harnessing waste heat, TEGs can contribute to power generation, enhancing the overall energy recovery process without requiring additional fuel consumption. This approach aligns with the industry's goals of increasing energy efficiency and minimizing greenhouse gas emissions, offering a sustainable solution for meeting growing energy demands. Furthermore, the economic analysis suggests that, while the initial investment may be substantial, the long-term savings and environmental benefits make this technology highly promising for the future of power generation. The findings could pave the way for broader adoption of TEG technology, encouraging the industry to explore innovative ways to maximize energy output while addressing environmental concerns.

## Acknowledgments

The authors would like to acknowledge the National Institute of Puducherry, Karaikal, India for the support to conduct this research.

Dr. Subbarama Kousik Suraparaju acknowledges the support of the UMPASA Post-Doctoral Fellowship.

**Funding:** This research was funded by the Ministry of Higher Education, Malaysia, and Universiti Malaysia Pahang Al-Sultan Abdullah (UMPASA) through the Fundamental Research Grant Scheme (FRGS): FRGS/1/2021/STG05/UMP/02/5 (UMPASA: RDU210126).

**Author contributions:** Subbarama Kousik Suraparaju: Conceptualization, Methodology, Formal analysis, Investigation, Data Curation, Writing - Original Draft. Elavarasan Elangovan: Formal analysis, Writing - Original Draft. Gopi Vasudevan: Methodology, Data Curation, Visualization. Mahendran Samyako: Resources, Writing - Review & Editing. Sendhil Kumar Natarajan: Conceptualization, Investigation, Resources, Writing - Review & Editing, Supervision, Funding acquisition.

**Disclosure statement:** The authors declare no conflict of interest.

## References

- [1] C.A. Gould, N.Y.A. Shammass, S. Grainger, and I. Taylor. A comprehensive review of thermoelectric technology, micro-electrical and power generation properties. In *2008 26th International Conference on Microelectronics*. IEEE, May 2008.
- [2] Subbarama Kousik Suraparaju, Gudapati Kartheek, Gummalla Venkata Sunil Reddy, and Sendhil Kumar Natarajan. A short review on recent trends and applications of thermoelectric generators. *IOP Conference Series: Earth and Environmental Science*, 312(1):012013, September 2019.
- [3] Mohammad Ameri, Omid Farhangian Marandi, and Behrouz Adelshahian. The effect of aperture size on the cavity performance of solar thermoelectric generator. *Journal of Renewable Energy and Environment*, 4(2):39–46, 2017.

- [4] Ssenoga Twaha, Jie Zhu, Yuying Yan, and Bo Li. A comprehensive review of thermoelectric technology: Materials, applications, modelling and performance improvement. *Renewable and Sustainable Energy Reviews*, 65:698–726, November 2016.
- [5] Wei He, Gan Zhang, Xingxing Zhang, Jie Ji, Guiqiang Li, and Xudong Zhao. Recent development and application of thermoelectric generator and cooler. *Applied Energy*, 143:1–25, April 2015.
- [6] Dongliang Zhao and Gang Tan. A review of thermoelectric cooling: Materials, modeling and applications. *Applied Thermal Engineering*, 66(1–2):15–24, May 2014.
- [7] M.D. Rowe, Gao Min, S.G.K. Williams, A. Aoune, K. Matsuura, V.L. Kuznetsov, and Li Wen Fu. Thermoelectric recovery of waste heat-case studies. In *IECEC-97 Proceedings of the Thirty-Second Intersociety Energy Conversion Engineering Conference (Cat. No.97CH6203)*, page 1075–1079 vol.2. IEEE, 1997.
- [8] RE Simons and RC Chu. Application of thermoelectric cooling to electronic equipment: a review and analysis. In *Sixteenth Annual IEEE Semiconductor Thermal Measurement and Management Symposium (Cat. No. 00CH37068)*, pages 1–9. IEEE, 2000.
- [9] Gao Min and D.M. Rowe. Experimental evaluation of prototype thermoelectric domestic-refrigerators. *Applied Energy*, 83(2):133–152, February 2006.
- [10] D. Astrain, A. Martínez, and A. Rodríguez. Improvement of a thermoelectric and vapour compression hybrid refrigerator. *Applied Thermal Engineering*, 39:140–150, June 2012.
- [11] A. R. Knox, J. Buckle, J. Siviter, A. Montecucco, and E. McCulloch. Megawatt-scale application of thermoelectric devices in thermal power plants. *Journal of Electronic Materials*, 42(7):1807–1813, February 2013.
- [12] Xiaolong Gou, Heng Xiao, and Suwen Yang. Modeling, experimental study and optimization on low-temperature waste heat thermoelectric generator system. *Applied Energy*, 87(10):3131–3136, October 2010.
- [13] Xiaolong Gou, Suwen Yang, Heng Xiao, and Qiang Ou. A dynamic model for thermoelectric generator applied in waste heat recovery. *Energy*, 52:201–209, April 2013.
- [14] Mauro Brignone and Alessandro Ziggotti. Impact of novel thermoelectric materials on automotive applications. In *AIP Conference Proceedings*. AIP, 2012.
- [15] Jeffrey W. Fergus. Oxide materials for high temperature thermoelectric energy conversion. *Journal of the European Ceramic Society*, 32(3):525–540, March 2012.
- [16] Duraisamy Sivaprahasam, Subramaniam Harish, Raghavan Gopalan, and Govindhan Sundararajan. *Automotive Waste Heat Recovery by Thermoelectric Generator Technology*. InTech, July 2018.
- [17] B. Orr, A. Akbarzadeh, M. Mochizuki, and R. Singh. A review of car waste heat recovery systems utilising thermoelectric generators and heat pipes. *Applied Thermal Engineering*, 101:490–495, May 2016.
- [18] T. Furue, T. Hayashida, Y. Imaizumi, T. Inoue, K. Nagao, A. Nagai, I. Fujii, and T. Sakurai. Case study on thermoelectric generation system utilizing the exhaust gas of internal-combustion power plant. In *Seventeenth International Conference on Thermoelectrics. Proceedings ICT98 (Cat. No.98TH8365)*, ICT-98, page 473–478. IEEE.
- [19] T. Kyono, R.O. Suzuki, and K. Ono. Conversion of unused heat energy to electricity by means of thermoelectric generation in condenser. *IEEE Transactions on Energy Conversion*, 18(2):330–334, June 2003.
- [20] H. Kaibe, K. Makino, T. Kajihara, S. Fujimoto, and H. Hachiuma. Thermoelectric generating system attached to a carburizing furnace at komatsu ltd., awazu plant. In *AIP Conference Proceedings*, page 524–527. AIP, 2012.
- [21] Marit Takla Børset, Øivind Wilhelmsen, Signe Kjelstrup, and Odne Stokke Burheim. Exploring the potential for waste heat recovery during metal casting with thermoelectric generators: On-site experiments and mathematical modeling. *Energy*, 118:865–875, January 2017.

- [22] W.B. Krueger and A. Bar-Cohen. Optimal numerical design of forced convection heat sinks. *IEEE Transactions on Components and Packaging Technologies*, 27(2):417–425, June 2004.
- [23] C.J. Shih and G.C. Liu. Optimal design methodology of plate-fin heat sinks for electronic cooling using entropy generation strategy. *IEEE Transactions on Components and Packaging Technologies*, 27(3):551–559, September 2004.
- [24] Liping Wang and Alessandro Romagnoli. Cooling system investigation of thermoelectric generator used for marine waste heat recovery. In *2016 IEEE 2nd Annual Southern Power Electronics Conference (SPEC)*, page 1–6. IEEE, December 2016.
- [25] Daniel Kraemer, Bed Poudel, Hsien-Ping Feng, J. Christopher Caylor, Bo Yu, Xiao Yan, Yi Ma, Xiaowei Wang, Dezhi Wang, Andrew Muto, Kenneth McEnaney, Matteo Chiesa, Zhifeng Ren, and Gang Chen. High-performance flat-panel solar thermoelectric generators with high thermal concentration. *Nature Materials*, 10(7):532–538, May 2011.
- [26] R. Amatya and R. J. Ram. Solar thermoelectric generator for micropower applications. *Journal of Electronic Materials*, 39(9):1735–1740, April 2010.
- [27] Hongxia Xi, Lingai Luo, and Gilles Fraisse. Development and applications of solar-based thermoelectric technologies. *Renewable and Sustainable Energy Reviews*, 11(5):923–936, June 2007.
- [28] Susant Kumar Sahu, Arjun Singh K, and Sendhil Kumar Natarajan. Electricity generation using solar parabolic dish system with thermoelectric generator—an experimental investigation. *Heat Transfer*, 50(8):7784–7797, July 2021.
- [29] Daniel Champier. Thermoelectric generators: A review of applications. *Energy Conversion and Management*, 140:167–181, May 2017.
- [30] K. M. Saqr, M. K. Mansour, and M. N. Musa. Thermal design of automobile exhaust based thermoelectric generators: Objectives and challenges. *International Journal of Automotive Technology*, 9(2):155–160, April 2008.
- [31] Jihui Yang and Thierry Caillat. Thermoelectric materials for space and automotive power generation. *MRS Bulletin*, 31(3):224–229, March 2006.
- [32] D.M. Rowe. Applications of nuclear-powered thermoelectric generators in space. *Applied Energy*, 40(4):241–271, January 1991.
- [33] J. Yang. Potential applications of thermoelectric waste heat recovery in the automotive industry. In *ICT 2005. 24th International Conference on Thermoelectrics, 2005*. IEEE, 2005.
- [34] Jihui Yang and Francis R. Stabler. Automotive applications of thermoelectric materials. *Journal of Electronic Materials*, 38(7):1245–1251, February 2009.
- [35] Z.B. Tang, Y.D. Deng, C.Q. Su, W.W. Shuai, and C.J. Xie. A research on thermoelectric generator’s electrical performance under temperature mismatch conditions for automotive waste heat recovery system. *Case Studies in Thermal Engineering*, 5:143–150, March 2015.
- [36] Saniya LeBlanc. Thermoelectric generators: Linking material properties and systems engineering for waste heat recovery applications. *Sustainable Materials and Technologies*, 1–2:26–35, December 2014.
- [37] Jack Philip Holman. *Experimental methods for engineers*. McGraw-Hill, 1971.
- [38] Mohana Krishna Peddojula, Subbarama Kousik Suraparaju, Mahendran Samykano, C.S. Vyasa Krishnaji Kadambari, Yasin Pathan, Afaf Zaza, V. Krishna Kanth, Reji Kumar Rajamony, Sendhil Kumar Natarajan, and Swapna Babu Budala. Synergetic integration of machining metal scrap for enhanced evaporation in solar stills: A sustainable novel solution for potable water production. *Thermal Science and Engineering Progress*, 51:102647, June 2024.
- [39] Subbarama Kousik Suraparaju, Mohana Krishna Peddojula, Mahendran Samykano, Mahmoud S. El-Sebaey, CS Vyasa Krishnaji Kadambari, Swapna Babu Budala, TN VV Ramkumar Manepalli, Lavanya Reddy, Sanjay Raju Vardhanapu, Bhogeswara Rao Ajjada, and Ramesh Babu Pilli. Enhancing the productivity of pyramid solar still utilizing repurposed finishing pads as cost-effective porous material. *Desalination and Water Treatment*, 320:100733, October 2024.